UNIVERSITY OF CALIFORNIA SAN DIEGO

Evaluation of a Smartphone-based Motion Capture System for Athletic Movement Screening

A Thesis submitted in partial satisfaction of the requirements for the degree Master of Science

in

Bioengineering

by

Rebecca Gow

Committee in Charge:

Professor Andrew D. McCulloch, Chair
Professor Daniela Valdez-Jasso
Professor Samuel R. Ward

2023

The Thesis of Rebecca Gow is approved, and it is acceptable in quality and Form for publication on microfilm and electronically.

University of California San Diego

2023

DEDICATION

To my mom, you inspire me every day to continue to achieve even when faced with challenging situations. I love you.

TABLE OF CONTENTS

LIST OF FIGURES

LIST OF TABLES

LIST OF ABBREVIATIONS

MOCAP - Marker-based motion capture
IMU - Inertial Measurement Unit
DVJ - Drop vertical jump
SL - Single leg
SD - Standard deviation
RMSE – Root mean square error

ACKNOWLEDGEMENTS

I would like to express my sincere gratitude to my primary advisor, Dr. Andrew McCulloch, for his constant feedback and reassurance throughout this journey. I would also like to thank Dr. Samuel Ward for his valuable constructive feedback and Dr. Daniela Valdez-Jasso for her encouragement throughout my time here at UCSD. Additionally, this work would not be possible without the funding support of the Wu Tsai Human Performance Alliance and Joe and Clara Tsai Foundation.

I would like to extend a special thanks to everyone at Rady Children's Hospital, especially Avery Takata and John Collins, for allowing us to use the lab space to conduct this study and helping to collect data. This work also would not have been possible without all the UCSD athletes that participated. I am grateful to Zach Weatherford for providing clinical feedback, helping to recruit athletes, and being so supportive of this work. Special thanks also to Dr. Susan Sigward for helping to conceptualize this research and spending so much providing clinical feedback.

I would also like to acknowledge all the Cardiac Mechanics Research Group members, especially Jen Stowe, Dr. Stephanie Khuu, Dr. Katie Knaus, Dr. Alex Noonan, Lisa Pankewitz, Marcus Hock, Berat Gulecyuz, and Yasser Abdelrahman for the chats, encouragement, and willingness to lend a hand whenever needed. Thank you for all the fun times! I also owe a great deal of gratitude to Dr. Swithin Razu for teaching me so much.

Lastly, I would be remiss in not mentioning my family and friends for the unconditional love and support throughout this journey. Words cannot express my gratitude for my fiancé, Brendan, for being there every step of the way and providing unwavering support. I would also like to thank my parents and my siblings for their encouragement and belief in me which kept my spirits and motivation high during this process.

ABSTRACT OF THE THESIS

Evaluation of Smartphone-based Motion Capture System for Athletic Movement Screening

by

Rebecca Gow

Master of Science in Bioengineering

University of California San Diego, 2023

Professor Andrew D. McCulloch, Chair

Marker-based motion analysis is used to evaluate human movement and identify biomechanical features related to injury risk. However, these studies require extensive expertise, are labor intensive, time consuming, and high cost, making them impractical for routine use. Open-source smartphone-based motion capture systems such as OpenCap offer scalable, low cost, and automated alternatives to conventional motion capture systems. The goal of this study was to compare OpenCap to gold standard clinical marker-based motion capture for movement screening tasks. Sixty-two retroreflective markers were placed on ten healthy collegiate female athletes who completed a set of tasks commonly used to assess movement quality. A musculoskeletal model was used to estimate hip adduction, hip flexion, hip rotation, knee flexion, and ankle flexion with both OpenCap and marker-based inverse kinematics. OpenCap was approximately 12 times faster for data collection and processing,

with only 2% of trials deemed unusable. RMSEs ranged from 3.5 to 11.3° across all joints and movement tasks. Pearson's correlation coefficients for peak joint angles for select movements ranged from moderate to very strong for hip, knee, and ankle flexion and weak to very strong for hip adduction and hip rotation. Bland Altman plots showed varying trends, bias, and limits of agreement depending on the movement and joint angle. This suggests that smartphone markerless motion capture offers a time and cost-effective alternative for capturing movement and should be further evaluated for suitability to specific clinical questions. Moreover, this platform can be further developed to increase accuracy with enhanced training of algorithms and become a standard tool for routine, high-throughput movement screening in athletes.

Chapter 1 INTRODUCTION

1.1 Overview of Movement Screening

Human biomechanics is the application of mechanical principles to understand the structure, function, and motion of the body on multiple scales, from the cell to whole organism level. At the whole organism level, biomechanics describes how the musculoskeletal system (muscles, bones, cartilage, ligaments, tendons, and connective tissues) responds to forces to generate movement (1). Voluntary movements create the adduction, abduction, flexion, extension, and rotation of joints relative to other joints. The quality of these movements is related to the subjective constructs of strength, flexibility, balance, and power. These constructs are pertinent to individual's participation in daily activities as well as recreational and elite sports (2).

Unsurprisingly, injuries such as ligament or muscle sprains, or suboptimal movement strategies, alter mechanical interactions between the components of the musculoskeletal system (1). These perturbations cause instability and changes to force distribution across tissues and joints, resulting in greater risk for injury or re-injury. Optimal movement strategies, thought to involve aligned joints, muscle coordination, and posture, reduce undesirable force on the musculoskeletal system and can help to prevent injury, speed up rehabilitation, and increase performance (3). It is therefore essential to evaluate musculoskeletal biomechanics during human movement and investigate how novel and previously identified features of movement relate to onset and progression of disease, injury prevention, and recovery (3–5). This project arose from the need for accessible and standardized measures of human movement screening, current state of the art tools for the study of movement and evaluates a subset of these tools for use in screening of previously identified fundamental movements patterns. Specifically, a scalable, open-source, and low-

cost smartphone camera system (OpenCap) is compared with gold standard marker-based motion capture (mocap) to measure lower limb kinematics of athletes completing a series of movement tasks commonly used to evaluate injury risk, return to sport status, or performance.

Assessing movement to understand disease status or to make clinical recommendations has existed in the medical field for decades and is now common practice (6–8). An early example of this application is the evaluation of walking patterns which has evolved into clinical gait analysis; a method routinely used to diagnose pathologies, improve rehabilitation, and aid clinical decision making following injury or neuromuscular insults such as stroke and cerebral palsy (9,10). Other standardized assessments of movement exist in the medical field to detect movement features associated with the severity of a disease or assess an individual's ability to function safely such as the 'timed up and go' test or the Unified Parkinson's Disease Rating Scale (UPDRS) (6,11).

In the past few decades, sports scientists and physiotherapists emulated the idea of movement screening to assess movement more objectively and systematically in an effort to draw conclusions or recommendations about readiness to compete or injury risk (2,12–17). Movement screens are also used to place athletes into appropriate training programs to mitigate injury risk and increase athletic performance. These movement assessments include isolated muscle or joint testing such as an isometric strength assessment, that capture specific information about the strength and mobility of focal regions (18). Athletic movement screens now also incorporate whole body testing to capture multi-segment or whole-body fundamental movement strategies that challenge the musculoskeletal system with more complex and higher load tasks (12). These movement screens are used to assess an individual's movement system and challenge the constructs of strength, flexibility, balance,

and power in an attempt to identify features that may put an athlete at risk for injury. Some of these movements and features associated with injury are discussed in the following section.

1.2 Clinical Relevance of Common Movements

Common movements used to evaluate whole body movement strategies include squat, single leg (SL) squat, drop vertical jump (DVJ), single leg drop vertical jump (SL DVJ), lunge, and a cutting maneuver among many others (3,19–21). Visual, kinetic, and kinematic parameters of the lower limbs during key phases of these movements are evaluated in these tasks to determine the quality of an individual's movements to either predict injury risk or help define return to sport. The scope of this work is to evaluate lower limb kinematics and therefore only relevant kinematic features of these movements are discussed. For example, a squat is a fundamental movement pattern in athletics. It has been proposed that the ability to perform a squat to 90° of knee flexion or more with proper symmetry and coordination is an indicator of optimal movement quality. This is because completing this movement requires stability and mobility from each of the major lower body joints: hip, knee, and ankle (2,3).

In an attempt to predict risk of Anterior Cruciate Ligament (ACL) injury, the dual limb and single limb drop vertical jump movement screens are used as a clinical evaluation of how an individual responds to increased force during the landing phase of these tasks. Subjects are evaluated on their ability to perform these movements stably and correctly either according to literature-based features of injury, or as compared to a healthy or contralateral limb (21–24). For example, discrete points during drop vertical jump movements are evaluated in the sagittal plane to estimate joint angles such as peak hip flexion, peak knee flexion, and peak ankle flexion. Insufficient flexion in females in the sagittal plane, especially hip and knee flexion, results in a stiff landing. This has been associated with an increased risk of injury as joint flexion is used to control the forces experienced at the knee during a landing

maneuver (23,25). When there is insufficient hip and knee flexion, the passive joint restraints such as the ACL take up a greater joint load to stabilize the knee. Therefore, limited range of motion in the sagittal plane is a risk factor for lower limb injury and is often studied during single or dual limb drop vertical jumps (26). For example, Pollard *et al* classified fifty-eight female athletes completing a dual limb drop vertical jump into peak low and high flexion groups. The study found that the low flexion group (67.4 ± 8.1° peak hip flexion, 86.5 ± 8.5° peak knee flexion) demonstrated increased knee valgus, increased knee adduction moments, and decreased energy absorption at the hip and knee compared to the high flexion group (27). Female athletes with this lower flexion biomechanical profiles may therefore be at a higher risk of ACL injury. Peak knee adduction has also been studied during a single limb drop vertical jump with greater than 5° of adduction categorized as abnormal and potentially associated with an increased risk of ACL injury. Increased hip adduction is also indicative of limited core strength and weak hip adductors (26,28).

Kinematic differences and asymmetries at discrete points are also observed in athletes returning to sport following an injury. These discrete points are assessed during a single leg squat, drop vertical jump, and single leg drop vertical jump in regards to functional disability in ACL-injured patients to help define return to sport and prevent re-injury as summarized in systematic reviews (24,29) and research studies (22,30). Examples of discrete points include peak knee flexion, peak hip flexion, and peak ankle flexion in addition to peak hip adduction for the single limb tasks. For example, Yamazaki *et al* evaluated the kinematics of female athletes returning to sport following an ACL injury with a single leg squat and found significant differences between the involved leg and both the uninjured leg and healthy controls (31). Restoring correct alignment of an ACL injured limb is expected to reduce ACL re-injury and assist in safe return to sport.

Kinematics have also been studied in relation to the development of patellofemoral pain (PFP), one of the most common lower extremity ailments (32). While little is known about the risk factors associated with the development of this disorder, it is postulated that excessive hip adduction and internal rotation are contributory to developing PFP (28). One prospective study also found that decreased knee flexion at initial contact and peak during a drop vertical jump was associated with increased risk of the development of PFP (33).

Kinematic differences are also observed in athletes with and without PFP. For example, one study found a significant difference in peak hip internal rotation during a drop jump, running, and step-down task in females with PFP vs pain free females (34). Another study evaluated kinematics during a single leg squat between males and females with and without PFP. The study found that females with PFP had greater peak hip internal rotation compared to the control group (35). Other studies have evaluated different features or additional discrete points in these movements, and other movements, such as range of motion or initial contact for a jumping task. Peak points of the movement are just one example of a likely important feature for further evaluation.

Movement screening of athletes is critical to identifying risk factors for injury as injuries can affect an athlete's quality of life in the long term. Research has shown that adolescents following a sports-related knee injury are more prone to functional deficits and are at a greater risk of being overweight/obese 3-10 years post injury compared to uninjured controls (36). Other studies have found that PFP causes knee pain 4 to 18 years after initial presentation causing restricted physical activity in some and may be associated with the development of patellofemoral osteoarthritis (33). Identification of movement features that may predispose athletes to injury is essential, and there are various tools that exist to help capture and examine these movement features.

1.3 Tools for Studying Movement

Various tools exist to assess athletes' movement strategies. Common tools include visual evaluations, inertial-measurement-units-based motion capture (IMUs), markerless motion capture, and marker-based motion analysis. Various accuracy and cost tradeoffs exist for each of these methods, the main points of which are summarized in Figure 1.1.

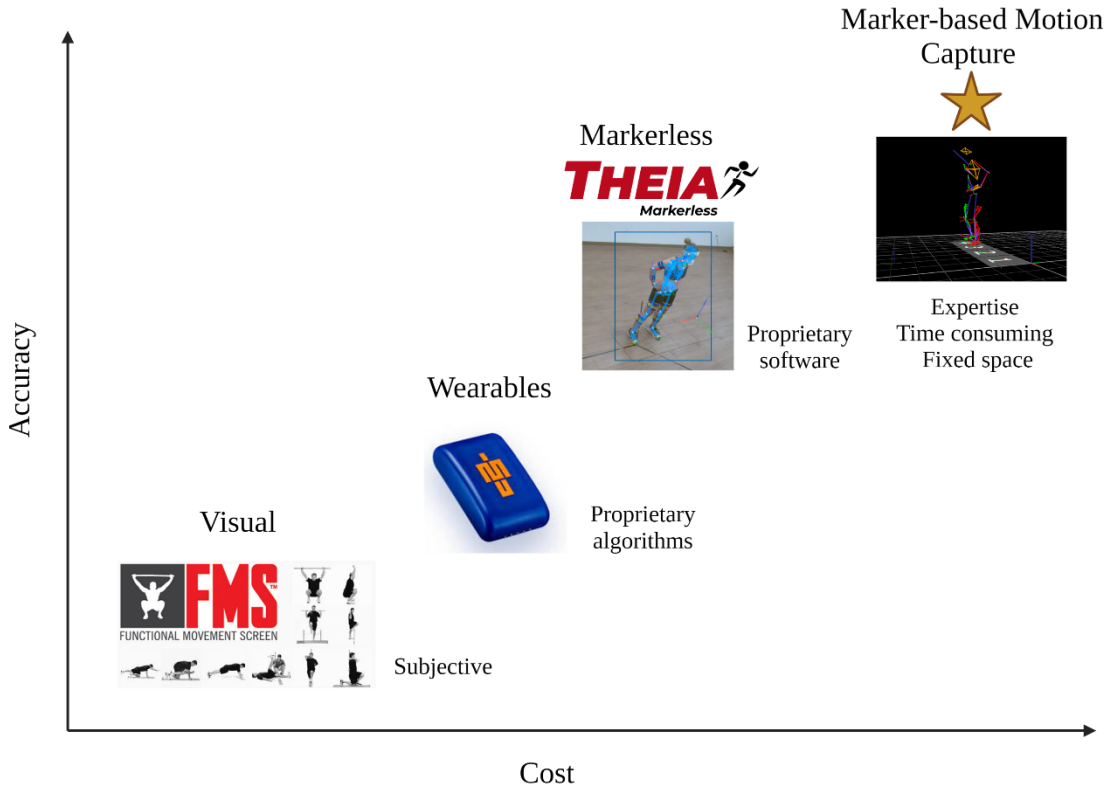

Figure 1.1: Comparison of common tools used to assess movement including visual, wearables, markerless, and mocap arranged according to relative cost and accuracy. The main limitations, besides cost, are also listed next to the technique.

1.3.1 Visual Tools

Visual evaluations are routinely used by strength and conditioning coaches to assess athletes' movements. These visual assessments can include singular tasks such as a drop vertical jump, or multicomponent movement screens such as the Functional Movement

Screen (FMS) or Movement Competency Screen (MCS) (2,3,37). The FMS consists of a series of tasks common to daily life that place individuals in extreme joint positions that highlight asymmetries and movement deficiencies and can easily be recognized by the assessor (2). Individuals are given a score from 0 to 3 based on the execution of each task. The MCS is a visual movement screen requiring no specialized equipment and consisting of a battery of tests common to sports. Athletes are given a score for each movement based on a number of criteria related to shoulder, lumbar, and knee movement (38). Points are deducted if the subject has rounded or elevated shoulders, rotated, hyperextended or hyper-flexed back or collapsed knees. The score on the movement screen aim to inform tailoring of training programs for reduction of injury risk (2,3,37).

Visual assessments are low cost and easy to implement; however, they are subjective due to their visual nature. The quality of the assessment is dependent on the training and previous knowledge of the practitioner, which is commonly the coach or trainer. As a result, test scores show weak interrater reliability (5,39). Other limitations of visual assessments include that differences between scores need to be large enough for a human eye to detect and scoring may not be specific enough to capture variability between individuals (40). Furthermore, the research correlating the outcome of visual movement assessments, primarily the FMS, to injury is variable due in part to the lack of objective and quantitative metrics such as kinematics and kinetics (15,39,41).

1.3.2 Gold Standard Marker-based Motion Capture

In a research setting, more quantitative and objective tools involving the measurement of biomechanical variables such as joint angles and muscle forces exist to study human motion. Mocap is considered the gold standard among these tools and, when combined with force plates and musculoskeletal models, it allows for more in-depth investigations into the

relationship between movement and injury. Additionally, mocap is able to detect much smaller differences in movement than what a human observer could perceive (21).

For example, a drop vertical jump can be evaluated in a motion capture lab to better define metrics such as a threshold of knee valgus, a value that may indicate an athlete's risk for ACL injury (43). However, while objective and accurate, traditional marker-based motion analysis is expensive, time consuming, labor intensive, requires expertise, and is effectively non-portable. A motion capture lab usually requires a fixed space and includes equipment costing more than $150,000 (44). Subject preparation for a capture session with retroreflective markers takes a trained clinician upwards of an hour and markers may impede athletes' natural motion (45). In addition, data processing can take several days for a trained expert such as a kinesiologist or engineer to complete. Therefore, mocap is largely limited to a research setting, with restricted scalability for conducting large scale studies to explore the relationship between movement and injury.

1.3.3 Wearables and Markerless

There has been a shift in the field of biomechanics to use more mobile and accessible tools to conduct larger scale studies due to the aforementioned limitations of traditional capture systems. Prospective large-scale studies are necessary for relating movement mechanics with injury risk factors. An example of portable, wearable technology are IMUs. These sensors contain an accelerometer, gyroscope, and often a magnetometer to enable on field capture of human movement over long periods of time (hours) (42). They are lightweight and unobtrusive enough to be worn during high intensity sport. One IMU each on adjacent segments is required to capture a joint angle, and only relative joint angles are obtained using IMUs. The accuracy of IMUs is varied and depends on signal processing characteristics and the application of interest (46,47). Furthermore, commercially available IMUs are expensive (~$2000/IMU) and utilize proprietary algorithms for sensor fusion which

limits the adaptability for unique studies. Currently, IMUs are primarily used to estimate kinematics; the algorithms to estimate kinetics using IMUs are still being explored and require high level expertise. OpenSense, an open-source toolbox for measuring joint angles with IMUs, may help to overcome some of these limitations surrounding cost and proprietary algorithms, but the validity of this with a wide range of movements and applications has not yet been explored (46).

Markerless motion capture systems including Kinect (Microsoft Corporation, WA, USA) and Theia3D (Theia Markerless Inc., Kingston, ON, Canada) have also gained popularity as more accessible and flexible systems. The Microsoft Kinect is a low-cost system that incorporates infra-red light and a video camera to track the position of the limbs. It also uses a depth sensor to create a 3D map and capture 3D movement patterns (47,48). The key limitations of the Microsoft Kinect relate to accuracy compared to mocap, scalability, and use outside of the lab. Inaccurate body tracking results when the Kinect is unable to distinguish between similar body parts or movements. Additionally, the system cannot easily be used outside of the lab due to poor performance in low light conditions and portability challenges (49).

Theia3D is a commercially available markerless motion capture system that uses machine learning to identify key points and automatically outputs a pose estimation of each joint. This system has been shown to accurately measure kinematics and shows promise for gait analysis. However, it requires a minimum of six synchronized cameras alongside high cost and proprietary software (50,51). Furthermore, while automated, this system is still yet to be streamlined or widely adopted, and, therefore, requires expertise to troubleshoot. There exists a need for a tool that bridges the gap between qualitative visual and quantitative traditional mocap assessments. The tool should remove the subjective nature of visual assessments, and the high cost associated with specialized equipment, proprietary software,

and extensive expertise for mocap. Furthermore, it should be able to capture larger differences in movement than a human eye. This tool would allow for large scale studies and aid coaches in obtaining more objective measurements in an athletic unconfined setting (i.e., out of the lab).

1.3.4 Smartphone-based Motion Capture System

OpenCap is a markerless smartphone-based motion capture system newly developed by Human Performance Lab at Stanford University. This system is a low cost, automated, and scalable platform for studying human movement. It utilizes between two and five iPhone cameras to collect synchronous data and provide kinematic, kinetic, and muscle activation outputs. These outputs are then processed and analyzed to provide a more objective and robust analysis of human motion as compared to a visual assessment. The system is also low cost compared to mocap, with data collection and processing feasible without a trained professional present (50). The accessibility of OpenCap is a critical consideration if it is to be clinically translatable, as many of the aforementioned biomechanical tools for studying human movement are prohibitively expensive, time-consuming, and require a higher level of expertise than many coaches and trainers have. For validation of OpenCap, Uhlrich *et al.* conducted multiple small-scale studies (n=10) of Opencap for sit to stand, gait, squat, and drop vertical jump movements. A larger scale study was also conducted to identify asymmetries in squats in a population of 100 subjects to demonstrate the scalability and ease of use of the technology. OpenCap development and function has been summarized in (50).

1.4 Study Introduction

The overall aim of this study was to compare motion capture using OpenCap with gold standard clinical maker-based motion capture for quantitative study of human movement

(kinematics) in female athletes. First, the usability of OpenCap was assessed. This was evaluated based on the data collection time including setup, subject instrumentation, and data processing time. Usability was also evaluated based on the percentage of failed OpenCap trials detected during data analysis. Next, a Root Mean Square Error (RMSE) across the movement cycle for common movement screening tasks was used to assess how accurately OpenCap was able to reproduce the gold standard measurement of kinematics. A generalized linear mixed effect model was constructed for each movement to identify sources of variation in the joint angle measures across technologies, joints, movement phase, replicate, and subjects. Next, a more detailed analysis of the differences across the movement phase was analyzed for representative movements. Finally, between-system correlation and agreement at discrete points was evaluated for movements that ranged in accuracies as described by the RMSEs and differences along the movement cycle. These movements included squat, single leg squat, drop vertical jump, single leg drop vertical jump, and lunge and twist. Data collection consisted of concurrent OpenCap and mocap of ten female athletes completing a series of common movement screening tasks described in Table 2.3.

Chapter 2 METHODS

2.1 Experimental Setup

Subjects

Ten female collegiate ground-based athletes from soccer (seven) and volleyball (three) who were free from injury volunteered to participate over an eight-month period. Anthropometrics are summarized in Table 2.1. Subjects were instructed to wear a sports bra or tight-fitting tank top, fitted high traction sneakers and shorts or compression shorts. All subjects read and signed informed consent approved by University of California San Diego Institutional Review Board (#804157).

Table 2.1: Summary of participants' anthropometrics.

Height	Mass	Age
1.72 ± 0.07 m	66.5 ± 12.9 kg	20 ± 1.2

Marker-based Motion Capture

62 retroreflective markers were placed on anatomical landmarks as shown in Figure 2.1. Acronyms are summarized in Table 2.2. The markers were affixed bilaterally on the scapula acromial edge, humerus, medial/lateral humeral epicondyle, radius styloid process, ulna styloid process, scapula inferior edge, anterior superior iliac spine, medial/lateral femoral epicondyle, medial/lateral prominence of the medial/lateral malleolus, calcaneus, first, second, and fifth metatarsal, and base of the first metatarsal. Markers were also affixed to C7, T10, and the suprasternal notch and a headband with four markers was worn. Rigid tracking clusters containing four markers each were affixed on the lateral part of the thighs and shanks about midway between the joint centers. One rigid tracking cluster containing three markers was placed on the lower back at the posterior superior iliac spine.

Table 2.2: Description of marker names and locations.

Marker Acronym	Marker Name/Location
R/L FHD	Right/Left Front Head
R/L SHO	Right/Left Shoulder
CLAV	Clavicle
R/L HLE	Right/Left Humerus Lateral Epicondyle
R/L UPA	Right/Left Upper Arm
R/L WRR	Right/Left Wrist Radius
R/L WRU	Right/Left Ulna
R/L FIN	Right/Left Finger
C7	C7
R/L SIA	Right/Left Scapula Inferior Angle
T10	T10
R/L ASI	Right/Left Anterior Superior Iliac
R/L PSI	Right/Left Posterior Superior Iliac
PELS	Pelvis Superior
R/L TH 1-4	Right/Left Thigh 1-4
R/L MFC	Right/Left Medial Femoral Condyle
R/L LFC	Right/Left Lateral Femoral Condyle
R/L SH 1-4	Right/Left Shank 1-4
R/L MMAL	Right/Left Medial Malleoli
R/L LMAL	Right/Left Lateral Malleoli
R/L HEE	Right/Left Heel
R/L SFOOT	Right/Left Superior Foot
R/L MTP5	Right/Left Metatarsal 5
R/L MTP2	Right/Left Metatarsal 2
R/L MTP1	Right/Left Metatarsal 1

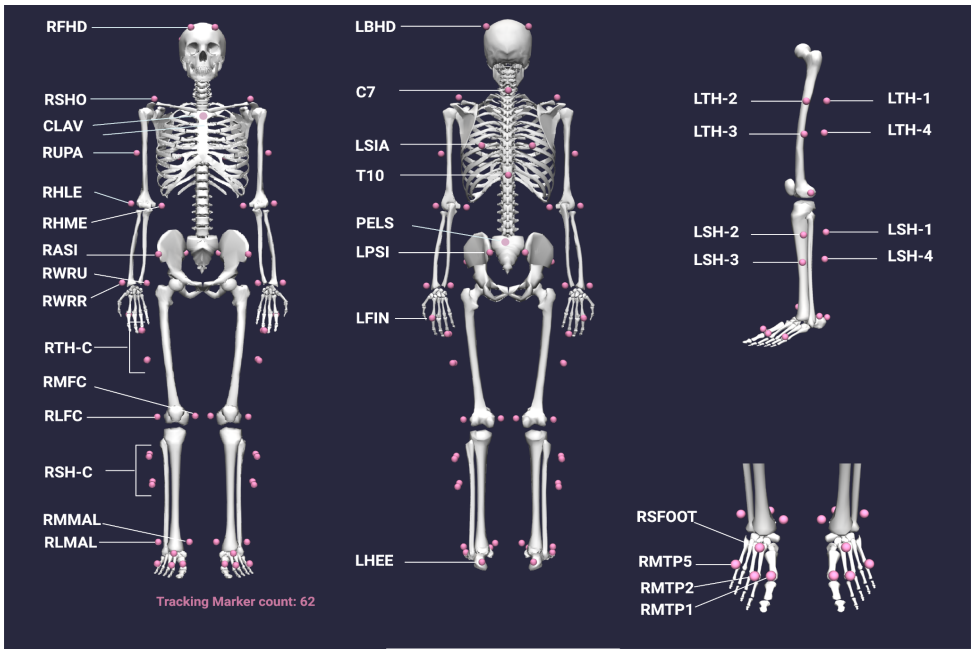

Figure 2.1A

Figure 2.1B

Figure 2.1: 2.1A lists the marker acronyms on a OpenSim model and 2.1B shows the marker positioning on a subject.

OpenCap

Two Opencap setups, each with three iPhone (model X, Apple, Cupertino, CA) cameras, were utilized depending on the tasks. The iPhones were connected to the OpenCap web application via a QR code, and then calibrated with a 210x175 mm, five rows, six columns, 35 mm square size checkerboard printed on A4 paper. The checkerboard was

affixed to a plexiglass surface and placed in a custom printed plastic stand that was orthogonal to the floor.

Setup one included three iPhones attached to hanging phone mounts about two feet apart from each other (Figure 2.2, left). The center camera was placed frontal to the subject and the two sides cameras were placed at approximately a 30-degree angle from the center camera. Setup two included two iPhones attached to hanging phone mounts and one center iPhone on a three-foot tripod each about two feet apart from each other (Figure 2.2, right). The center camera was placed frontal to the subject and the two sides cameras were placed at about a 30-degree angle from the center camera. The tasks that involved vertical movement were captured during session one with setup one and the tasks that involved forward motion (i.e., broad jump and lunge) were captured during session two with setup two.

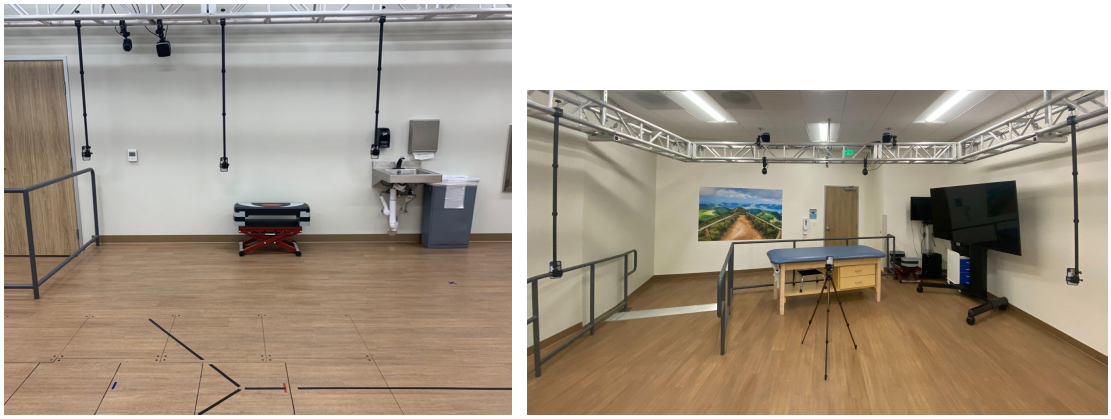

Figure 2.2: OpenCap setups. Setup one is shown on the left and setup two is shown on the right.

2.2 Experimental Data Collection

The prescribed subject warmup was jogging, skipping, high knees, and buttkicks across the length of the lab back and forth 1 time, in addition to 3 squats, 3 countermovement jumps, 3 lateral shuffles, 3 broad jumps, 3 45-degree cuts, and 3 decelerations. Following subject marker placement and preparation, the subjects completed the prescribed warmup.

Three-dimensional (3D) kinematic data was collected using a 10-camera (Miqus, Qualisys AB, Göteborg Sweden) motion capture system at 120 Hz. Cameras were arranged in an approximately 35 feet x 25 feet rectangular space. Qualisys track manager (QTM) was used to synchronously collect data with all ten cameras. A static pose with the subject in a motorbike position (Figure 2.3, left) and a trial capturing range of motion was collected from each subject. OpenCap data was collected at 60 Hz and a static pose with the subject in an A frame (Figure 2.3, right) was collected to calibrate the OpenCap system.

Figure 2.3: Mocap static pose and OpenCap static pose.

Subjects practiced each of the movement tasks three times at 60%, 75%, and 100% effort. A description of each movement task can be found in Table 2.3.

Table 2.3: Summary of movement tasks.

Movement	Uni- or Bilateral	Description
Squat	Bilateral	Hands on side of head, squat as low as possible then come right back up.
Single Leg Squat	Unilateral	Hands on side of hips, squat as low as possible with one leg back, and then come right back up.
Countermovement Jump	Bilateral	Hands on hips, go down, and then jump as high as possible in one smooth motion.
Single Leg Countermovement Jump	Unilateral	Hands on hips, with one leg back, go down, and then jump as high as possible in one smooth motion
Heel Touch	Unilateral	Stand on an 8-inch box with hands on hips, squat down with one leg and lightly tap the floor with the heel of the contralateral limb then come back up to standing.
Drop Vertical Jump	Bilateral	Stand on a 30-cm box, hop forward and land on both feet at the same time. Then, immediately jump as high as possible, using arms for momentum.
Single Leg Drop Vertical Jump	Unilateral	Stand on a 30-cm box, hop forward and land on one foot. Then, immediately jump as high as possible, using arms for momentum.
Lateral Shuffle	Unilateral	Shuffle to the side 4 meters without crossing the feet until the lead foot hits the marked square, then shuffle back to the starting point as fast as possible.
Lunge and Twist	Unilateral	Cross arms and place hands on shoulders with elbows pointing out. Perform a forward lunge and rotate into the lead leg. Return to center and then push back to return to starting position.
Single Leg Broad Jump	Unilateral	Jump horizontally on one leg as far as possible and stick the landing
45 Degree Cut	Unilateral	Run forward 4 meters and then plant and turn 45 degrees
Deceleration	Unilateral	Run forward 4 meters and then plant and backpedal 4 meters
Y-Balance Test	Unilateral	Stand on one leg and reach anteriorly, posteromedially, and posterolaterally

Following practice, each movement task was captured with both mocap and OpenCap. Data collection procedures are shown in Figure 2.4. Refer to the Appendix for the full data collection protocol.

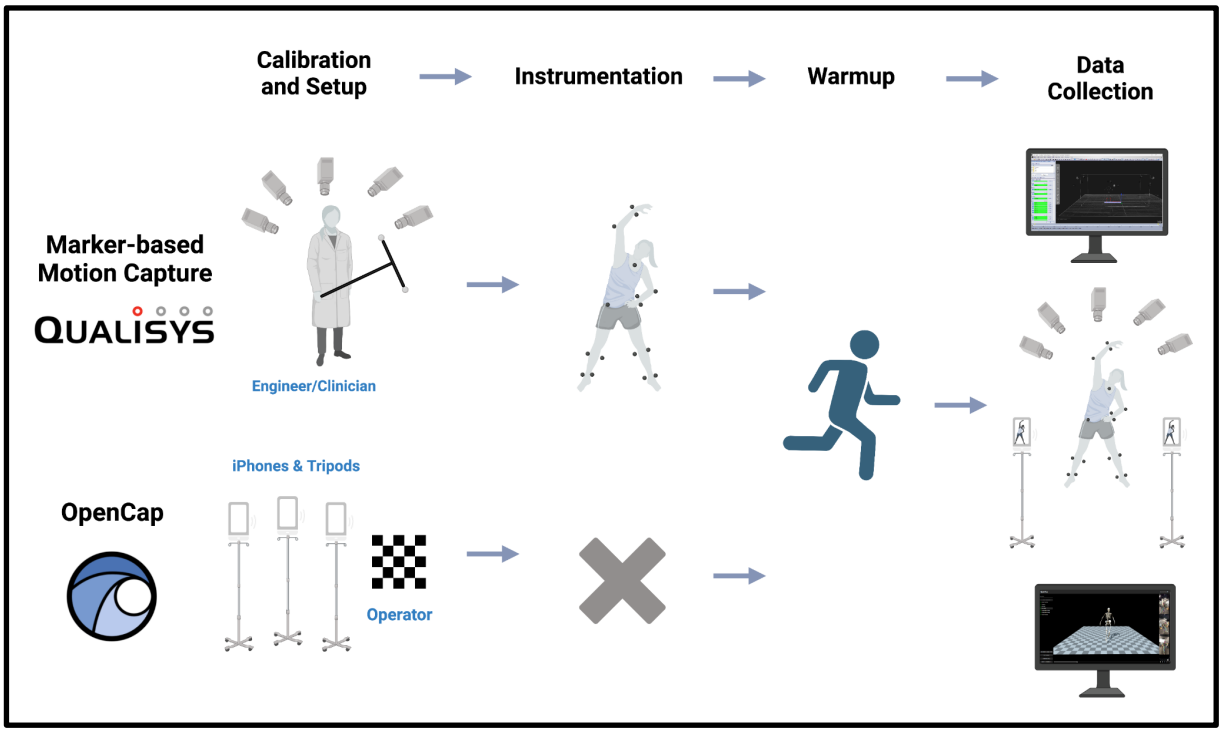

Figure 2.4: OpenCap and mocap setup, subject instrumentation and warmup, trial collection.

2.3 Data Processing

Marker-based Motion Capture

The mocap data was labeled and gap filled. The start and end of each trial was then identified and the data was processed through Addbiomechanics software to obtain kinematics (52). This process is summarized in Figure 2.5 and described in more detail in the following subsections.

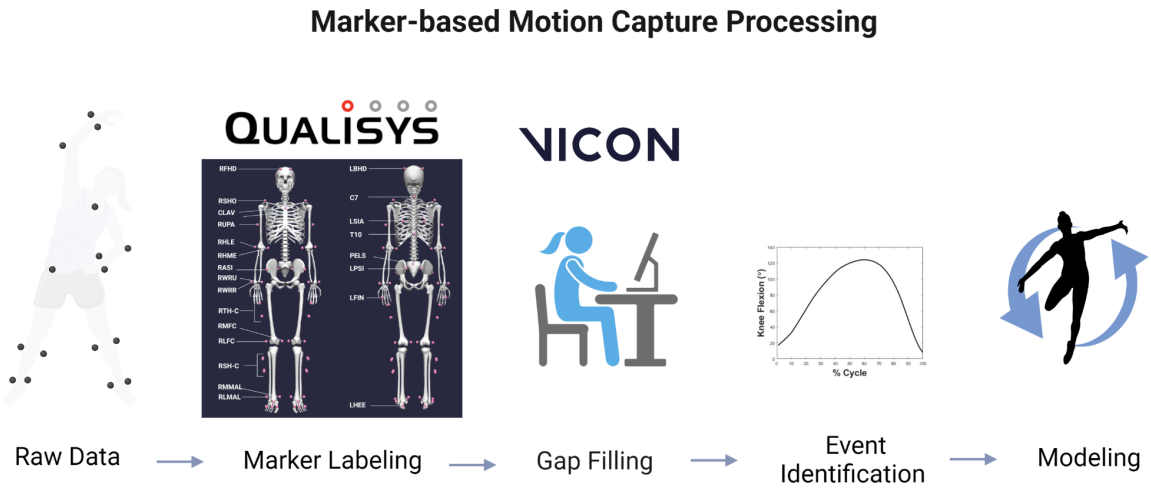

Figure 2.5: Marker-based motion capture processing steps include marker labeling of the raw data, gap filling of missing marker trajectories, identification of start and stop events for each movement, and finally modeling using Addbiomechanics to obtain kinematics.

Qualisys Track Manager

Three-dimensional kinematic data was first processed in QTM to associate retroreflective markers with anatomical locations and remove false markers created during data reconstruction that do not represent actual marker trajectories. Data was reconstructed with two infrared cameras that triangulated the 3D position of a marker to provide the location and trajectory. A label list was created to identify and name the markers on the subject. The trial capturing range of motion for each subject was then manually labeled and added to an Automatic Identification of Markers (AIM) model. An AIM model is used to automatically identify and label markers and track all types of motion. The AIM model is a learning model that is improved each time a new subject is added to it with different dimensions. The AIM model was then used to automatically label markers for the movement trials. Each trial was checked for accuracy in labeling by overlaying the markers on the video data and ensuring the labels were associated with the correct anatomical segment. All ghost markers created during reconstruction were deleted by overlaying the marker trajectories on

the video data and visually comparing the locations. Trials were exported in a .C3D format for processing in Vicon Nexus (Vicon, Oxford, UK).

Vicon Nexus

Trial .C3D files were imported into Vicon Nexus where markers were relabeled using a custom automated labeling skeleton. Gaps in marker trajectories were then filled using a combination of methods: spline fill, pattern fill, and rigid body fill. Spline fill is a cubic spline interpolation and was used for gaps less than five frames. Pattern fill uses the shape of another similar trajectory to fill a gap. This type of fill was often used for the hand, wrist, and feet markers. A rigid body fill can be used when a rigid or semi-rigid relationship exists between four or more markers. This was the primary type of gap fill used.

Following gap filling, a conventional gait model was implemented to obtain lower limb joint angles (hip, knee, ankle) and events (start/stop) were identified using certain features of each movement (53). The features used for events for each movement are summarized in Table 2.4 and further description can be found in the Appendix.

After events were identified, the data was filtered using a 4th order, zero lag, Butterworth filter at 4 Hz for squat, single leg squat, heel touch, lunge and twist, and Y balance test and 30 Hz for the remaining movements (43,54). The data was exported as a .trc which contains the time series trajectory data (x, y, and z) for each marker.

Table 2.4: Description of the features used to identify the start and end of each movement.

Movement	Start	End
Squat	Largest increase in slope of knee flexion before ascent	Largest decrease in slope of knee flexion following descent
Single Leg Squat	Largest increase in slope of knee flexion before ascent	Largest decrease in slope of knee flexion following descent
Countermovement Jump	Point before angular velocity of PELS marker crosses z axis into negative before ascent	Point after angular velocity of PELs marker crosses z axis into positive following absorption
Single Leg Countermovement Jump	Point before angular velocity of PELS marker crosses z axis into negative before ascent	Point after angular velocity of PELs marker crosses z axis into positive following absorption
Heel Touch	Point before angular velocity of PELS marker crosses z axis into negative before ascent	Termination of contact with force plate (10N threshold)
Drop Vertical Jump	Initial contact with force plate (10N threshold)	Point after angular velocity of PELs marker crosses z axis into positive following absorption
Single Leg Drop Vertical Jump	Initial contact with force plate (10N threshold)	Point after angular velocity of PELs marker crosses z axis into positive following absorption
Lateral Shuffle	Initial contact with force plate of lead leg (10N threshold)	Termination of contact with force plate (10N threshold)
Lunge and Twist	Initial contact with force plate of lead leg (10N threshold)	Termination of contact with force plate (10N threshold)
Single Leg Broad Jump	Largest increase in slope of knee flexion before ascent	Minimum vertical position of PELS marker following landing
45 Degree Cut	Initial contact with force plate of lead leg (10N threshold)	Termination of contact with force plate (10N threshold)
Deceleration	Initial contact with force plate of lead leg (10N threshold)	Termination of contact with force plate (10N threshold)
Y-Balance Test	Point before angular velocity of PELS marker crosses z axis into negative before first reach	Point after angular velocity of PELs marker crosses z axis into positive after final reach

Addbiomechanics

Addbiomechanics, an optimizer hosted by Stanford University, was used to process the marker-based motion capture data (52). Addbiomechanics optimally scales an OpenSim model and then estimates inverse kinematics. A Lai Arnold Opensim model with approximate marker locations was uploaded to Addbiomechanics. Markers on anatomical locations such as the anterior superior iliac spine were fixed, but tracking markers such as the upper arm marker were not fixed, and the position of these markers was optimized in Addbiomechanics. The .trc data for each trial was also uploaded along with subjects' height (with shoes), mass, and sex.

Using the input marker data, Addbiomechanics finds the functional joint centers, and then uses this to estimate an initial body segment scaling and marker location. Then, anthropometric covariance statistics (height, weight, sex) are used as a prior for helping to choose likely scaling of bones. The statistics come from the ANSUR II dataset which includes 93 measures for over 6,000 US military personnel (4,082 men and 1,986 women). Finally, a bilevel optimization problem is solved to match the model position to the experimental data as closely as possible. The final output from Addbiomechanics is a scaled model with registered markers and kinematics over the time course of each uploaded trial (52). This automatic processing of the data achieved a marker error (RMSE) range of 1.38 to 3.42 cm across the evaluated tasks and ten subjects. The largest errors were not specific to one task or one subject.

OpenCap

The OpenCap data processing workflow is shown in Figure 2.6. The steps include camera calibration, pose detection, synchronization, triangulation, marker augmentation, and OpenSim pipeline. Camera calibration requires setup and input from the user, but the

remaining processing steps all take place automatically in the cloud and therefore do not add any hands-on time for the user.

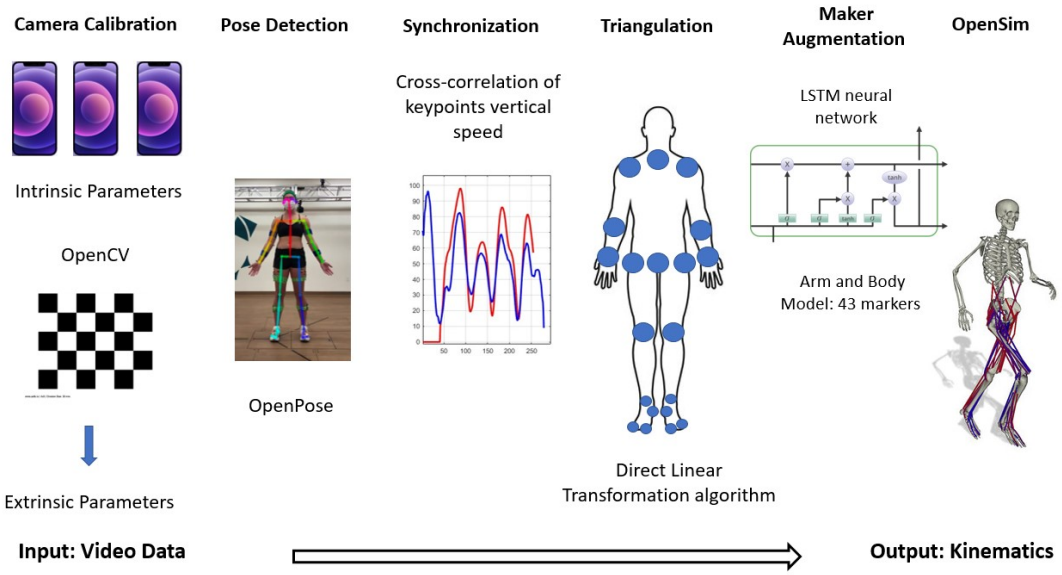

Figure 2.6: Steps for OpenCap data processing. The user calibrates the cameras during data collection and then the remaining steps take place in the cloud and include pose detection, synchronization, triangulation, marker augmentation, and modeling in OpenSim.

For calibration, the intrinsic parameters (principal point, focal length, and distortion parameters) of the three iPhones used were loaded from a database of pre-computed parameters related to the latest iPhone models by scanning a QR code. The three iPhones then took a still image of a checkerboard of known size. The intrinsic parameters and OpenCV, an open-source computer vision library used for extracting and processing data from images, was then used to automatically compute the extrinsic parameters from the image of the checkerboard. The extrinsic parameters indicated where the cameras were in space relative to each other and the checkerboard, specifically the camera transformation relative to the global frame where the origin was the bottom left corner of the checkerboard.

The pose detection algorithm, OpenPose, was used to identify 2D key points on the subject. OpenPose was trained on a set of annotated publicly available still images covering over 400 human activities including sports, walking, hiking, and bicycling. To help increase

the accuracy of the pose detection algorithm, OpenCap implements a bounding box to track the person of interest. Last, full body poses are assembled and output with 135 possible key points on the human body, foot, hand, and face. The pose detection algorithm also returned a relative confidence between 0 and 1 for each key point position (55). OpenCap uses these confidence scores to help identify occlusions and then uses cubic splines to replace the occluded key point positions. From the 135 key points identified with OpenPose, OpenCap uses 20 for further analysis which include the neck, mid-thigh, left/right shoulders, hips, knees, ankles, heels, small and big toes, elbows, and wrists.

Video recording on the three iPhones was not precisely synchronized because the connection between the iPhones and the web application was internet based. Therefore, additional steps were taken to ensure synchronization between cameras. First, the activity was detected to determine which synchronization function to use. Gait was identified by a large maximum cross correlation between the right and left ankle key points and a time delay of 0.1-1s. Specifically, a Gaussian curve dependent on the framerate is multiplied by the correlation plot helping to choose the smallest shift value for periodic motions. Gait trials were then synchronized by finding the delay that results in the lowest error between reprojected 3D key points and 2D video key points of the right and left ankle. Trials where a hand punch was identified, meaning one hand was quickly moved above the shoulders and brought down, were synchronized using the time delay that corresponded to the maximum cross correlation of the summed vertical speeds of the wrist and shoulder key points from all the cameras. Non-gait trials with no hand punch were synchronized using the time delay that corresponded to the maximum cross correlation of the summed vertical speeds of all the key points from all the cameras.

The 2D positions of the markers were then triangulated to get 3D positions using a direct linear transformation algorithm. Two long short-term memory networks (LSTM) were

used to augment a marker set from the 3D key points to define rotational planes of kinematic motion. An arm model was trained to predict the position of eight arm markers from nine arm and torso key points. A body model was trained to predict the position of 35 body makers from 13 lower-limb and torso key points. The total marker set includes 43 markers on upper and lower extremity bony landmarks and tracking markers on the thighs and shanks. The LSTM networks were trained on 108 hours of motion capture data which included running, walking, cutting, and jumping tasks (54).

The marker data was then fed through a traditional OpenSim pipeline to estimate kinematics. First the subjects' segments were scaled to minimize the distance between the experimental (augmented) markers and the model markers. For example, the tibia was scaled in the X (anterior/posterior), Y (superior/inferior), and Z (medial/lateral) direction using a scaling factor computed from the distance between the experimental and model marker at the knee joint center and the marker at the ankle joint center. All segments were scaled in one direction except for the pelvis and torso which were scaled in two directions, meaning one or two scaling factors were computed and applied to the remaining directions.

The OpenSim inverse kinematics tool was then used to estimate the joint angles. This process stepped through each time point and positioned the model in a pose that best matched the experimental marker locations. The tool uses a weighted least squares problem to mathematically determine the pose that minimizes both marker and coordinate error. During data collection, OpenCap used OpenPose at default resolution (308 x 368 pixels). To increase accuracy, the data was reprocessed with a higher resolution OpenPose (567 x 1008 pixels). This was implemented from a local instance of OpenCap and initiating a reprocess in the cloud with the higher resolution. Data was reprocessed as it was collected between January 17, 2023 and March 15, 2023 using the Opencap-core repository (56). Differences between subjects may exist due to continuous updating of the repository.

Biomechanical Model

The same constrained musculoskeletal model (Lai Arnold model) was used to obtain kinematics for both mocap and OpenCap. The model had 33 degrees of freedom (pelvis in the ground frame [6], hips [2x3], knees [2x1], ankles [2x2], metatarsophalangeal joints [2x1], lumbar [3], shoulders [2x3], and elbows [2x2]). Table 2.5 summarizes the model joint excursions for the lower limb extremity angles that were analyzed. This model is driven by 80 muscles that actuate the lower limb coordinates, 13 ideal torque motors that actuate the lumber, shoulder, and elbow coordinates, and six contact spheres per foot that model the foot ground contacts (43,57) .

Table 2.5: OpenSim Lai Arnold model lower limb joint excursions.

	Ankle Flexion	Knee Flexion	Hip Flexion	Hip Adduction	Hip Rotation
Lower (°)	-50	0	-30	-50	-40
Upper (°)	50	140	120	30	40

Data synchronization

The OpenCap and mocap data were synchronized using MATLAB signal processing toolbox (The MathWorks Inc., Natick, MA) to identify signatures in the data. First, the OpenCap data was up sampled from 60 Hz to 120Hz to match the frequency of the motion capture data. A delay was then calculated between the two signals using cross-correlation of knee flexion. The delay was then used to time-synchronize the OpenCap data with the mocap data and then the OpenCap data was cropped to the event cycles identified with mocap. Data from both systems was then interpolated to 101 data points (0-100%).

Generalized Linear Mixed Model

A generalized linear mixed effect model was fit to the data for each movement to understand what factors contributed the most variability. All analyses were conducted using SAS studio (SAS Institute Inc.) This model was used to account for fixed and random effects and was able to handle missing replicates. The response was continuous, and the residuals followed a univariate gaussian distribution for every movement, so therefore the general equation for the model is:

$$y = X\beta + Z\gamma + \varepsilon \tag{2.1}$$

where:

y is the n x 1 vector of observations,

β is a p x 1 vector of fixed effects,

γ is a q x 1 vector of random effects,

ε is a n x 1 vector of random error terms,

X is the n x p design matrix for the fixed effects relating observations y to β,

Z is the n x q design matrix for the random effects relating observations y to γ.

In the model, the joint angle value at each time point for each technology was the dependent response variable (y), time, joint, replicate, and technology were fixed effects and subject was a random effect. All two-way interactions and the three-way interactions of technology, time and replicate and technology, joint and replicate were considered. The three-way interaction of technology, time and joint was not considered due to lack of computational power to converge on a solution with the relatively large size data set. Therefore, the specific equation for the model is:

$$Joint\ Angle = \beta_1 * Technology + \beta_2 * Time + \beta_3 * Joint + \beta_4 * Replicate + \beta_5 * Technology * Time + \beta_6 * Technology * Joint + \beta_7 * Technology * Replicate + \beta_8 * Time * Joint + \beta_9 * Joint * Replicate + \beta_{10} * Time * Replicate + \beta_{11} * Technology * Joint * Replicate + \beta_{12} * Technology * Replicate * Time + \gamma_1 * Subject + \varepsilon \quad (2.2)$$

Time refers to the normalized phase of the movement and included values from 1-100, joint was a categorical variable and included left and right hip flexion, hip adduction, hip rotation, knee flexion, and angle flexion, replicate was either 1, 2 or 3 except in the cases where a replicate was missing, and technology was a categorical variable and included either OpenCap or mocap. Left and right joint angles for single limb tasks were combined. Subject (A15-A24) was a random effect because there may be a different outcome if a different group of people were selected for the study. The significance level, alpha, is equal to 0.05.

2.4 Data Analysis

The accessibility and usability of OpenCap was evaluated using four metrics: time, cost, expertise, and flexibility. Time was defined as the total time it took to collect and process data. Cost was defined as the total cost of materials to collect and process data. Expertise was defined as the skill level needed to collect and process data. Flexibility was defined as the ability to collect data in different spaces (i.e., out of the lab, capture volume, etc.) and data storage. The reliability of OpenCap was also evaluated based on the number of failed trials identified during data processing.

To assess the accuracy of OpenCap, Root Mean Squared Error (RMSE) was calculated. RMSE measures the average difference between values predicted by a model (OpenCap) and the actual values (gold standard motion capture). The variability between

OpenCap and mocap was also explored along with the average differences measured between the technologies across the movement cycle.

Kinematics at discrete points were evaluated using a Pearson's correlation coefficient (r) as a measure of the strength of the correlation between the two measurement technologies at the discrete points. The strength of the correlation as assessed by Pearson's correlation coefficient (r) was classified as very strong (0.90–1.00), strong (0.70–0.89), moderate (0.40–0.69), weak (0.10–0.39) or negligible (0.00–0.10) (58,59). The Bland-Altman method was also used to evaluate the mean bias and limits of agreement between OpenCap and mocap at the discrete points (60). Peak knee flexion, hip flexion, ankle dorsiflexion, hip adduction/abduction, and hip rotation were evaluated for a single leg squat, squat, drop vertical jump, single leg drop vertical jump, and lunge. These points were identified during the descent phase of the squat and single leg squat, initial contact to takeoff for the drop vertical jump and single leg drop vertical jump, and throughout the movement cycle for the lunge for the leading leg (61–63).

Chapter 3 RESULTS

3.1 Usability

The accessibility of Opencap was compared with the Qualysis mocap system used in this study. It required approximately 2.0 hours to collect and process OpenCap data per subject for a trained operator vs. 23 hours for mocap with a kinesiologist and engineer. OpenCap cost approximately $925 and can be used anywhere with wifi vs over $350,000 for mocap in a fixed lab space (Table 3.1). In terms of dependability, only 2% of OpenCap trials were unusable as identified during data analysis.

Table 3.1: Summary of the accessibility of mocap vs. Opencap. OpenCap takes less time, costs less, and does not require extensive training to obtain kinematics. OpenCap can be used anywhere with wifi.

	Qualisys Motion Capture	OpenCap
Cost	Upfront: $350,000 Yearly: $7000	$925 Optional: $5000
Expertise	Kinesiologist and/or engineer	Trained operator for kinematics (Engineer for kinetics)
Flexibility	Dedicated lab space	Anywhere with wifi
Time/subject	23 hours	2 hours

Cost

The Qualysis mocap system used in this study included ten Arqus infrared cameras, four AMTI in-ground force plates, a Qualisys track manager (QTM) software license, and a set of 62 retroreflective markers. The total estimated upfront cost for the system and software was $350,000. In addition, a service contract for QTM must be purchased to continue receiving software updates, which costs $4000 per year and there are Qualisys camera

warranties that cost an estimated $300 per camera per year (e.g., $3000/year for 10 cameras). The retroreflective markers must be secured to the subjects with disposable adhesive tape for each data collection, with estimated yearly replacement depending on the frequency of use. Retroreflective markers cost $70 for a set of ten markers (B&L Engineering).

The OpenCap system included a set of six tripods (2 setups), phone mounts, and three iPhones. The calibration checkerboard was printed on regular computer paper and taped to a piece of plexiglass which was put into a custom designed and 3D printed stand for a nominal cost. The OpenCap collection software was free to use and could be run on any operating system with no special requirements such as a graphics processing unit (GPU). The iPhones, tripods and phone mounts combined for a total cost of $925. The data was also reprocessed at a higher resolution to help increase accuracy which required a 3090 GPU (approximately $5000); however, this additional cost is not required to use OpenCap. There are no service contracts or disposables required to collect or process data.

Expertise

The motion capture system required extensive expertise for data collection and processing. Correct marker placement is critical as the accuracy of mocap directly relates to this. A kinesiologist was required to place markers on anatomically correct positions of each subject. A clinician or engineer is then required to set up, calibrate, and run the software during data collection to ensure high quality data. Similar expertise is also required to process the data.

OpenCap data collection can be set up and run by a trained operator. Kinematics are automatically processed and stored in the cloud and are easily downloaded for local analysis. However, while no expertise is required to obtain kinematics, prior knowledge of muscle driven simulations is required for simulating kinetics, which is a future direction of this study.

The settings (e.g., weights of the different terms in the optimal control problem), constraints, and cost function terms must be optimized to generate meaningful simulation results. The optimal solution will drive the model to closely match the measured kinematics while satisfying the dynamic equations and minimizing muscle effort. For example, different mesh densities and convergence tolerances must be tested to determine the influence on the results.

Flexibility

The marker-based motion capture system was not portable and required a dedicated lab space. The ten-camera system used for this study was set up in an approximately 800 ft^2 space. The OpenCap system can be set up anywhere, for example, an athletic setting, however wifi is required to collect data. The OpenCap capture volume for this study ranged from approximately 200-500 ft^2 depending on the setup and not all movements could be captured due to the constraints of the lab space. For example, a lateral shuffle was included in this study, but the capture was unsuccessful because this movement required the subject to move in and out of the capture volume. In terms of data size, each subject required about 100 GB of local storage for the raw mocap data, including the video data, which is necessary to accurately label markers. Whereas all the OpenCap data was stored in the cloud for easy data sharing and when downloaded locally, each subject required approximately one to two GB of storage.

Time

The time required to use each system can be divided up into setup, collection, and processing time. The setup time for Qualysis was approximately 90 minutes and included turning on cameras, calibrating cameras, and adhering markers to a subject in anatomically correct locations. Data collection took approximately one minute per trial, but varied

depending on the length of the movement for a total time of 1.5 hours per subject. Each data collection included approximately 72 trials (23 movements, three trials each plus functional range of motion and static calibration poses) that required processing. Processing time took between 16 - 20 hours to label and gap fill the markers and 3 - 4 hours to identify events and export data per subject (~72 trials). Addbiomechanics was used to scale and estimate kinematics, which reduced processing time by days. The estimated total time for setup, data collection, and data processing per subject was 23 hours of hands-on time. This could be reduced in future with more automated methods.

In contrast, the setup time for OpenCap was approximately 30 minutes. There was no subject preparation for this system. Data collection took the same amount of time as for mocap; about one minute per trial but varied depending on the length of the movement for a total time of about 1.5 hours per subject. Data processing for kinematics was automated in the cloud. The estimated total time for setup, data collection, and data processing was two hours per subject.

Reliability

All subjects completed at least three repetitions of each movement during data collection. Twenty-two extra mocap trials across the ten subjects and 15 analyzed movements (6 unilateral) were collected to obtain three successful mocap trials. During data analysis, OpenCap trials were marked as a failure if there were spikes in the data or if part of the trial was not captured. This resulted in fewer than three trials for some movements. One subject for right single leg squat was omitted entirely, and only two successful trials were included for the following: one subject for right single leg squat, two subjects for left drop vertical jump, one subject for right countermovement jump, and one subject for countermovement

jump due to poor capture quality for these specific trials. In total, eight of the 450 successful mocap trials were not usable for OpenCap, which is approximately 2% of trials.

3.2 Accuracy

Qualitative Comparison

Figure 3.1 shows representative mean ± standard deviation (SD) waveforms from ten subjects for the right lower limb joint angles (hip flexion, knee flexion, ankle flexion, hip abduction/adduction, and hip rotation) across the cycle of a squat for both mocap and OpenCap. These waveforms show that the OpenCap data demonstrated similar shape, trend, and magnitude of the joint angles as mocap data. Synchronicity of the waveforms was evaluated by the alignment of the peaks for knee flexion across the cycle of the movement for OpenCap and mocap.

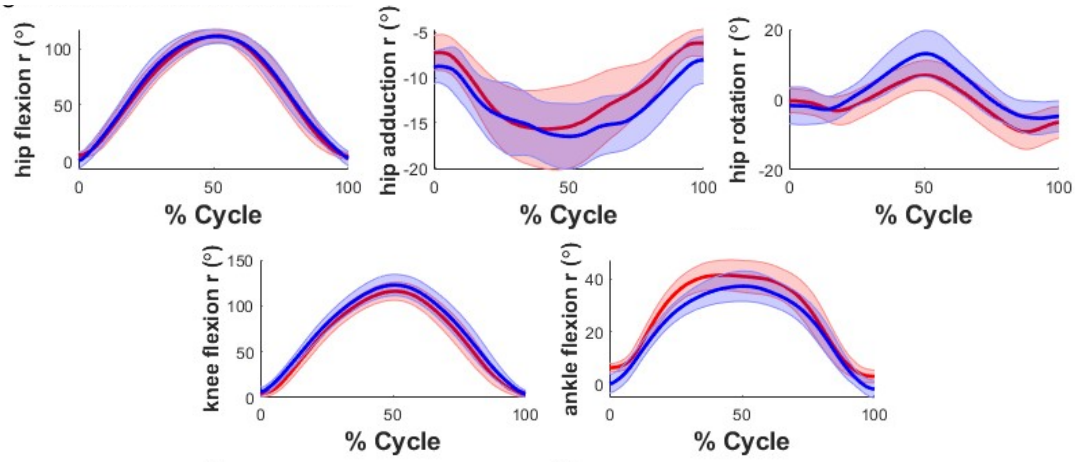

Figure 3.1: Mean ± SD waveforms (n=10 subjects) from mocap (blue), and OpenCap (red) for right lower limb joint angles.

Quantitative Comparison

RMSE of the lower limb joint angles between marker-based mocap and OpenCap was used to evaluate the accuracy of OpenCap across the cycle of each movement and assess how

well OpenCap was able to reproduce the gold standard mocap results. The metric provides an estimate of accuracy and indicates how well OpenCap predicted the true value (motion capture). Table 3.2 summarizes the average RMSE across the cycle of selected movements averaged across ten subjects and right and left limbs. Three trials are included for each movement except the ones mentioned previously and an additional missing right single leg squat trial due to operator error collecting the wrong limb.

Table 3.2: Summary of RMSEs for lower limb kinematics of each movement task between mocap and OpenCap. Note the RMSE for each limb are averaged. The percentage shown is the error as a percentage of the total range of motion for the specific task (joint excursion).

		Ankle Flexion [°]	Knee Flexion [°]	Hip Flexion [°]	Hip Adduction [°]	Hip Rotation [°]
OpenCap Setup 1	Squat	5.1 (14%)	7.3 (6%)	5.7 (5%)	3.5 (35%)	4.4 (27%)
	Single Leg Squat	8.1 (27%)	5.3 (8%)	10.6 (14%)	4.3 (29%)	5.4 (45%)
	Counter-movement Jump	10.4 (15%)	6.6 (7%)	7.4 (11%)	3.6 (17%)	5.1 (42%)
	Single Leg Counter-movement Jump	11.0 (18%)	7.0 (17%)	8.4 (14%)	4.7 (18%)	5.0 (45%)
	Heel Touch	9.0 (33%)	9.4 (14%)	7.6 (15%)	8.4 (29%)	6.2 (82%)
	Drop Vertical Jump	11.3 (17%)	6.6 (7%)	5.7 (7%)	3.6 (20%)	4.7 (29%)
	Single Leg Drop Vertical Jump	11.0 (19%)	8.1 (13%)	7.1 (19%)	5.1 (34%)	5.9 (60%)
OpenCap Setup 2	Lunge and Twist	9.3 (27%)	10.0 (13%)	10.8 (19%)	7.6 (33%)	5.4 (39%)
	Broad Jump	9.1 (21%)	7.6 (14%)	7.3 (13%)	5.6 (28%)	7.9 (100%)

Overall

The RMSE ranged from 3.5 - 11.3° for all lower limb joints and tasks between mocap and OpenCap. Ankle flexion RMSE ranged from 5.1 to 11.3° for all the movements and was the largest for jumping tasks (countermovement jump, drop vertical jump, and broad jump), ranging from 9.1 to 11.3°. Knee flexion RMSE ranged from 5.3 to 10° with the largest RMSE for lunge and twist and the smallest for single leg squat. Hip flexion RMSE ranged from 5.7 to 10.8° with the largest RMSE for lunge and twist and the smallest for drop vertical jump and squat. Hip adduction RMSE ranged from 3.5 to 8.4° with the largest for heel touch and the smallest for squat. Hip rotation RMSE ranged from 4.4 to 7.9° with the largest for single leg broad jump and the smallest for squat. The average RMSE in the frontal and transverse plane were smaller than the average RMSE in the sagittal plane.

In terms of the percent joint excursion, the RMSE ranged from 6 to 100%. The joint excursion was the average total range of motion for each movement in each plane as measured with mocap. For ankle flexion, percentage joint excursion RMSE ranged from 15% to 33% with the greatest percentage for heel touch and the smallest percentage for squat. For knee flexion, percentage joint excursion RMSE ranged from 6% to 17% with the greatest percentage for single leg countermovement and the smallest percentage for squat. For hip flexion, percentage joint excursion RMSE ranged from 5% to 19% with the greatest percentage for single leg drop vertical jump and lunge and twist and the smallest percentage for squat. For hip adduction, percentage joint excursion RMSE ranged from 17% to 35% with the greatest percentage for squat and the smallest for countermovement jump. For hip rotation, percentage joint excursion RMSE ranged from 27% to 100% with the greatest for broad jump and the smallest for squat.

3.3 Generalized Linear Mixed Model

The first few rows of an Analysis of Variance (ANOVA) table for the squat are shown in Table 3.3 as an example of how the data was set up for the analysis. This ANOVA table was repeated for each movement task and consisted of about 60,000 data points per movement.

Table 3.3: Example setup of the ANOVA table for a squat.

Technology	Joint	Subject	Time	Replicate	Value
'Mocap'	'hip_flexion_r'	'A15'	1	1	-4.87648
'Mocap'	'hip_flexion_r'	'A15'	1	2	-5.7044
'Mocap'	'hip_flexion_r'	'A15'	1	3	-6.41008
'Mocap'	'hip_flexion_r'	'A15'	2	1	-1.99433

The null hypothesis is that the factors do not significantly affect the joint angle values. Fixed effects where there were no significant differences ($p > 0.05$) include technology for broad jump and countermovement jump, replicate for single leg squat, the two-way interaction between technology and replicate for all movements except heel touch, the two-way interaction between replicate and time for broad jump, lunge, single leg drop vertical jump, and heel touch, the two-way interaction between technology and time for the single leg squat, the three-way interaction between technology, time and replicate for all movements, and the three-way interaction between technology, joint, and replicate for squat, countermovement jump, single leg countermovement jump, drop vertical jump, and broad jump. The remaining fixed effects and multi-way interaction effects were found to have a significant effect on the joint angle value ($p < 0.05$).

For all the movements, the most variability as indicated by the largest F-values, and p less than 0.05, can be attributed to joint, time, and the two-way interaction between

technology and joint. The F-value is a measure of the ratio of variance described by the model to the variance not described by the model, which is the ratio of the mean sum of squares for the model to the mean sum of squares error. A large F value indicates that the between group variation is larger than the within group variation. In all cases the covariance estimate for the random subject effect is non-zero and there are multiple subjects per movement with a significant p value. The results for each movement are shown in the Appendix.

3.4 Differences across Movement Cycle

Figure 3.2 shows the mean ± SD for hip flexion, hip abduction/adduction, hip rotation, knee flexion, and ankle flexion across the cycle of representative movements: squat, single leg squat, drop vertical jump and single leg drop vertical jump. The black line shows the mean ± SD difference between mocap and OpenCap across the cycle of each movement. Positive indicates hip adduction and internal rotation and negative indicates hip abduction and external rotation. Only the right limb is shown for the tasks for simplicity except for the single leg squat where the left limb is shown due to missing trials with the right single leg squat. The plots for the remaining movements are shown in the Appendix.

Figure 3.2: Mean ± SD waveforms (n=10 subjects) from mocap (blue), and OpenCap (red) for hip flexion, hip abduction/adduction, hip rotation, knee flexion, and ankle flexion across the movement cycle of a squat (A), single leg squat (B), single leg drop vertical jump (D), and drop vertical jump (C). The black line with shading indicates the mean ± SD between-system difference across the cycle of the movement.

A

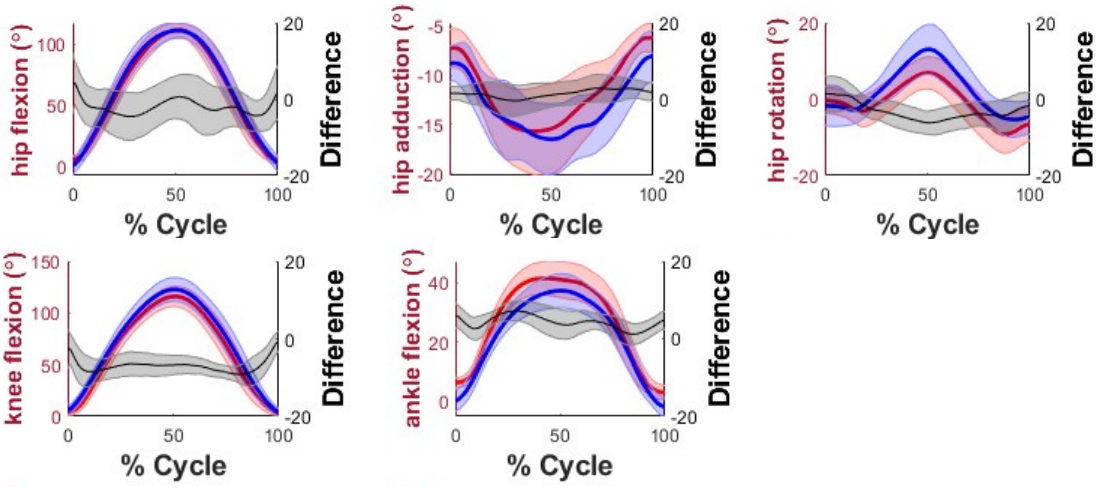
hip flexion (°)
hip adduction (°)
hip rotation (°)
knee flexion (°)
ankle flexion (°)
% Cycle
Difference

B

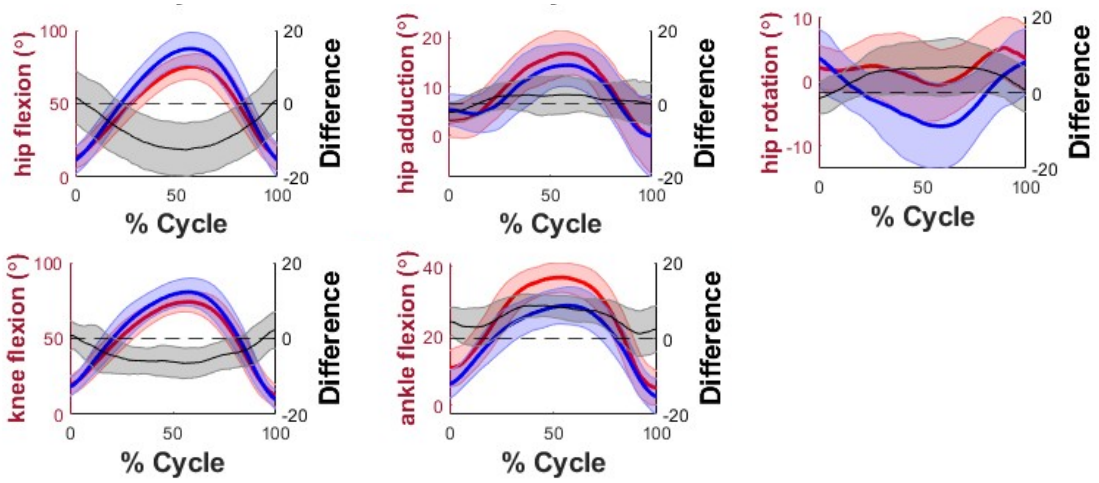
hip flexion (°)
hip adduction (°)
hip rotation (°)
knee flexion (°)
ankle flexion (°)
% Cycle
Difference

C

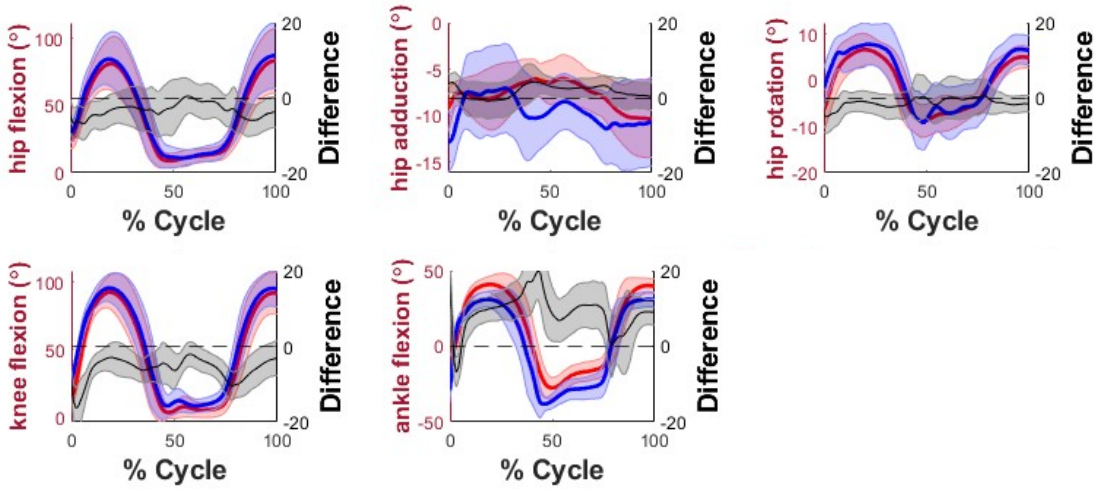
hip flexion (°)
hip adduction (°)
hip rotation (°)
knee flexion (°)
ankle flexion (°)
% Cycle
Difference

Figure 3.2, Continued.

D

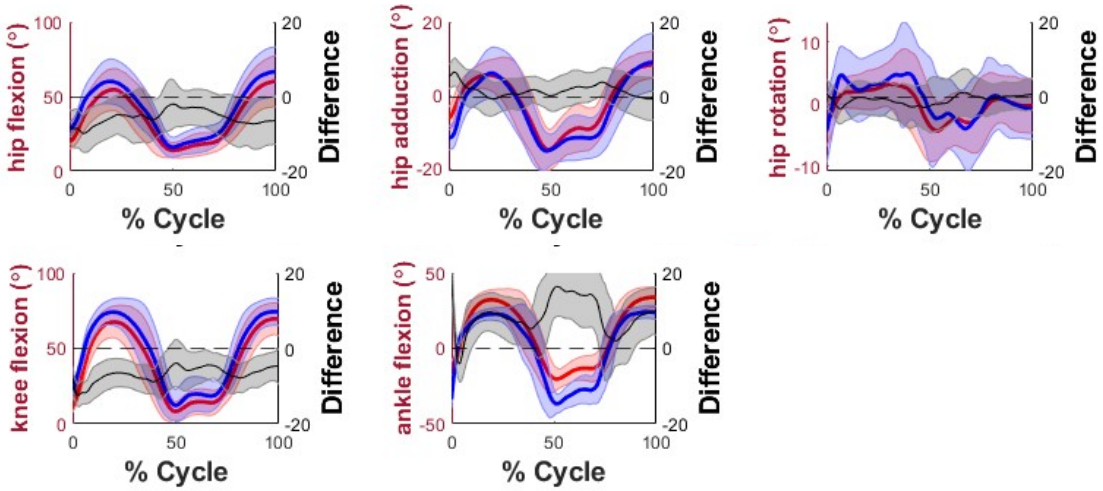

Dual Limb Squat

Figure 3.2A shows the dual limb squat waveforms for OpenCap and mocap and the average between-system differences across the movement cycle. The mean difference in hip flexion between the two systems ranged from -4.5 ± 6.3° to 4.2 ± 5.5° with the largest difference at approximately 25% of the cycle. For knee flexion, the mean differences ranged from -9.2 ± 2.2° to -0.6 ± 2.5° with larger differences present in the middle of the cycle (i.e., at deeper flexion). For ankle flexion, the mean differences ranged from 1.2 ± 2.8° to 7.2 ± 2.5°. For hip abduction, mean differences ranged from -0.1 ± 4.3° to 2.9 ± 3.6°. For hip rotation, mean differences ranged from approximately -6.2 ± 3.1° to 1.3 ± 4.7° with larger differences present with increasing external hip rotation (more negative). Hip flexion had the most variation in average differences indicated by the larger standard deviation reported and shown by the shading in Figure 3.2A. Knee flexion had the largest between-system differences.

Single Leg Squat

Figure 3.2 B shows the single leg squat waveforms for OpenCap and mocap and the average between-system differences across the movement cycle. The mean difference in hip flexion between the two systems ranged from -12.5 ± 7.2° to 1.6 ± 7.2° and the magnitude of the difference increased with increasing hip flexion. For knee flexion, the mean differences ranged from -6.5 ± 4.0° to 2.2 ± 4.8° and the magnitude of differences increases with increasing knee flexion. For ankle flexion, the mean differences ranged from 1.4 ± 6.0° to 8.7 ± 2.8° with larger differences at increased dorsiflexion. For hip adduction, the mean differences ranged from -2.3 ± 2.7° to 2.4 ± 5.2° with the largest differences during the descent phase of the movement (0 to 50%). For hip rotation, mean differences ranged from -1.2 ± 4.2° to 6.8 ± 7.5° with larger differences with increasing hip internal rotation. Hip

flexion had the most variation in the average between-system difference indicated by the larger standard deviation reported and shown by the shading in Figure 3.2B. Hip flexion also had the largest between-system differences.

Drop Vertical Jump

Figure 3.2C shows the drop vertical jump waveforms for OpenCap and mocap and the average between-system differences across the movement cycle. The mean difference in hip flexion between the two systems ranged from -7.0 ± 4.4° to 0.4 ± 4.7° with the greatest differences at initial and secondary contact with the ground which occur at 0% and approximately 80% of the movement phase, respectively. For knee flexion, the mean differences ranged from -16.2 ± 4.2° to -2.1 ± 4.5° with the largest differences around initial contact which occurs at the beginning of the movement phase. For ankle flexion, the mean differences ranged from -6.8 ± 4.2° to 20.0 ± 6.1° with the largest differences during initial contact and takeoff which occur at about 0% and 50% of the movement phase, respectively. For hip rotation, the mean differences ranged from -5.1 ± 4.5° to 0.5 ± 4.6° with the largest differences at initial contact. All the joints had larger between-system differences at initial contact. Ankle flexion had the largest between-system differences.

Single Leg Drop Vertical Jump

Figure 3.2D shows the single leg drop vertical jump waveforms for OpenCap and mocap and the average between-system differences across the movement cycle. The mean difference in hip flexion between the two systems ranged from -10.0 ± 5.1° to -2.0 ± 6.6° with the largest differences around initial contact which occurs at the beginning of the movement phase, around 0-5%. For knee flexion, the mean differences ranged from -12.4 ± 3.1° to -3.9 ± 6.3° with the largest differences around initial contact. For ankle flexion, the

mean differences ranged from approximately -4.1 ± 4.9° to 20.0 ± 6.6° with the largest differences at initial contact and during flight which occurs from about 50 to 70% of the movement cycle. For hip adduction, the mean differences ranged from approximately -0.7 ± 5.8° to 6.6 ± 3.7° with the largest differences at initial contact. For hip rotation, the mean differences ranged from approximately -3.2 ± 4.2° to 1.1 ± 6.4° with the largest differences at initial contact. Ankle flexion had the largest between-system differences.

3.5 Discrete Points

Discrete points of movement tasks were evaluated for a squat, single leg squat, drop vertical jump, single leg drop vertical jump, and a lunge. The discrete points evaluated include peak knee flexion, hip flexion, hip adduction, hip rotation, and ankle flexion at various points in the movement cycle depending on the task.

A summary of Pearson's correlation coefficients of the peak points between the two measurement systems are shown in Table 3.4. There was a very strong correlation at peak knee flexion for all movement tasks ranging from 0.9 to 0.98 except the lunge where the correlation is strong (0.88). There was very strong correlation at peak hip flexion for the jumping tasks (drop vertical jump and single leg drop vertical jump) ranging from 0.94 to 0.95, while there was strong correlation for the single leg squat (0.76) and lunge (0.85) and moderate correlation for the dual limb squat (0.57). There was a strong correlation for ankle dorsiflexion for all tasks ranging from 0.73 to 0.82 except the single leg drop vertical jump where the correlation is moderate (0.67). There was varying correlation for hip adduction for all tasks: moderate for single leg squat (0.41), strong for single leg drop vertical jump (0.74), and negligible for lunge (0.05) and varying correlation for hip abduction: moderate for squat (0.6) and weak for drop vertical jump (0.26). There was also varying correlation for hip

rotation: very strong for squat (0.92), strong for drop vertical jump (0.77), moderate for single leg drop vertical jump (0.42) and lunge (0.68) and weak for single leg squat (0.34).

Table 3.4: A summary of Pearson's correlation coefficients of discrete variables for knee flexion, hip flexion, ankle flexion, and hip adduction captured with mocap and OpenCap. The correlations are shown for squat, single leg squat, drop vertical jump, and single leg drop vertical jump. The strength of the correlation as assessed by Pearson's correlation coefficient (r) was classified as very strong (0.90–1.00), strong (0.70–0.89), moderate (0.40–0.69), weak (0.10–0.39) or negligible (0.00–0.10).

	Knee flexion	Hip flexion	Ankle flexion	Hip adduction	Hip rotation
Squat	0.98	0.57	0.79	0.6 (abduction)	0.92
SL Squat	0.9	0.76	0.79	0.41	0.34
DVJ	0.95	0.98	0.82	0.26 (abduction)	0.77
SL DVJ	0.93	0.93	0.67	0.74	0.42
Lunge	0.88	0.85	0.73	0.05	0.68

Bland Altman plots for each of the movements and discrete variables are shown below. This graphical representation describes the agreement of mocap and OpenCap for measuring a variable through the mean difference between both systems (bias), and the upper and lower 95% limits of agreement (64). A positive bias is present when OpenCap overestimated a joint angle compared to mocap and negative bias is present when OpenCap underestimated a joint angle compared to mocap. Limits that are closer to the bias suggest greater agreement between the two systems.

Figure 3.3 shows the Bland Altman plots of the discrete variables for the various movement tasks. Table 3.5 summarizes the bias and limits of agreement that correspond with Figure 3.3. Each set of colored dots represents a subject. There was clustering of each subject. For all movements, knee flexion was underestimated ranging from -2.6 to -11.1°. For squat, single leg squat, and single leg drop vertical jump, the bias was approximately -6.5°. OpenCap estimated a greater angle of dorsiflexion compared to a smaller angle captured by

mocap. The mean bias ranged from 4.5 to 9.7°. The single leg drop vertical jump, drop vertical jump, and lunge all had a mean bias of approximately 9.5°. Hip flexion was underestimated in all cases except for a dual limb squat. The bias ranged from -3.6 to -12.5° in cases where hip flexion was underestimated whereas the bias is 0.6° for the squat. Hip adduction bias ranged from -0.1 to 2.3° for the single limb tasks whereas hip abduction ranged from -1.0 to 1.1° for the dual limb tasks. Hip rotation bias ranged from -0.5 to 7.2° and was always underestimated for internal hip rotation: -2.6 to -6.2° for drop vertical jump and squat. The LOA were the largest for the single leg squat and the smallest for the drop vertical jump across all the movements.

Figure 3.3: Bland-Altman representations comparing the differences between OpenCap and mocap at discrete points. The x axis of these plots is the peak value for mocap joint angle and the y axis shows the difference in peak joint angle in degrees between OpenCap and mocap. The dashed-dotted line represents the mean bias between the measurements made between both systems. The red dashed horizontal lines represent the 95% limits of agreement.

A

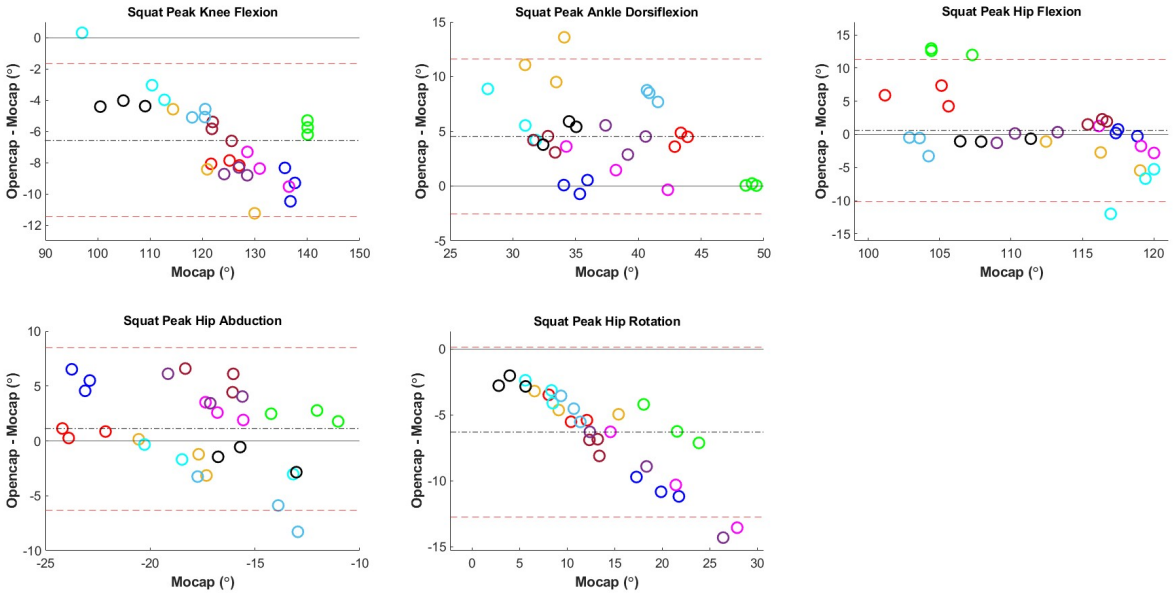
Squat Peak Knee Flexion
Squat Peak Ankle Dorsiflexion
Squat Peak Hip Flexion
Squat Peak Hip Abduction
Squat Peak Hip Rotation
Opencap - Mocap (°)
Mocap (°)

B

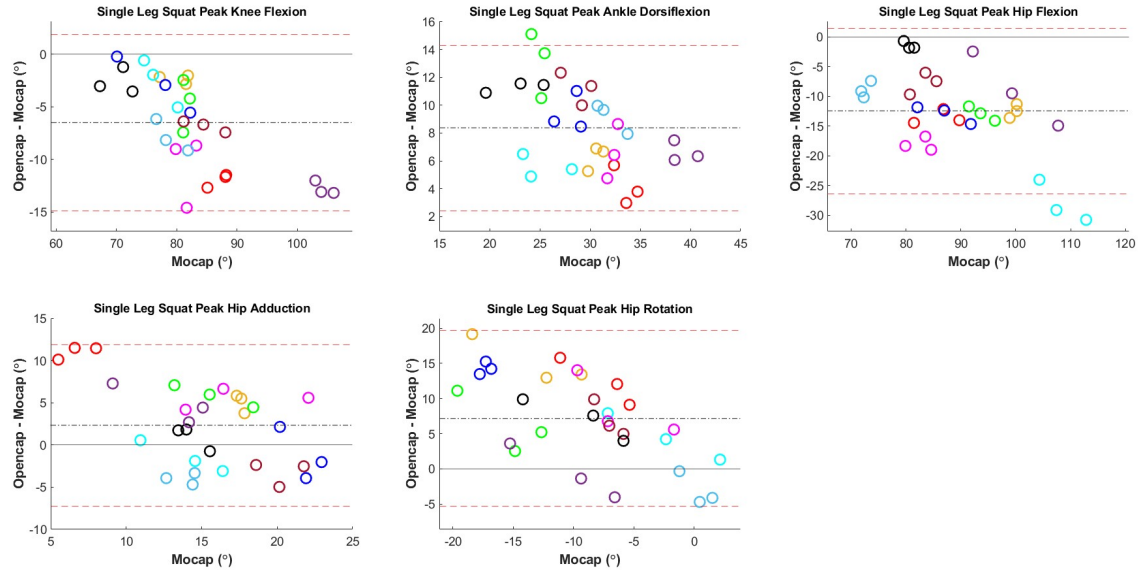
Single Leg Squat Peak Knee Flexion
Single Leg Squat Peak Ankle Dorsiflexion
Single Leg Squat Peak Hip Flexion
Single Leg Squat Peak Hip Adduction
Single Leg Squat Peak Hip Rotation
Opencap - Mocap (°)
Mocap (°)

Figure 3.3, Continued

C

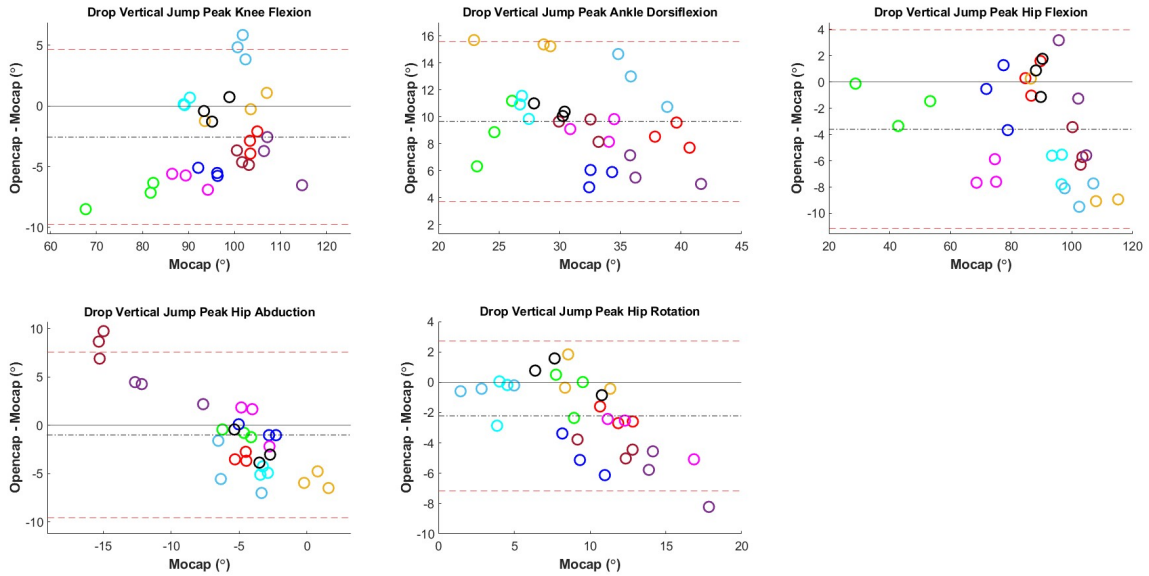

D

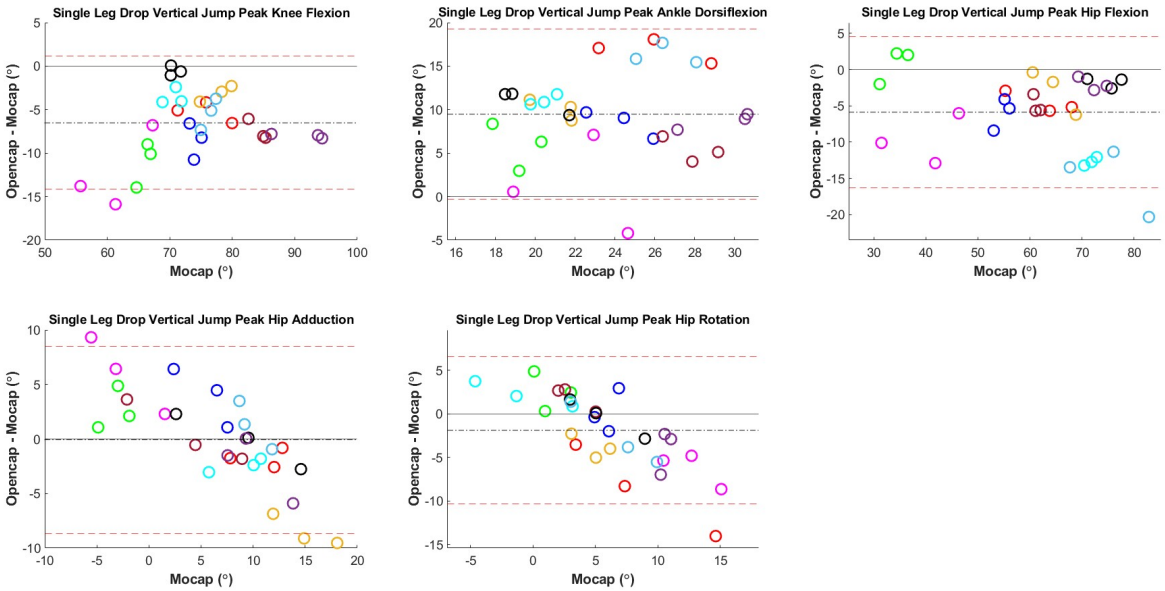

Figure 3.3, Continued

E

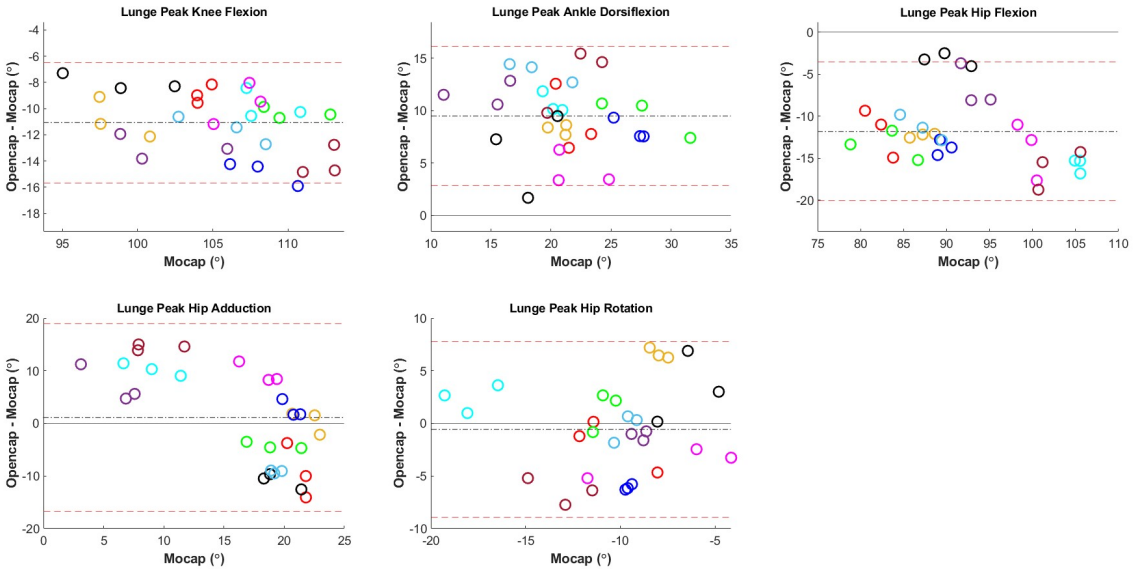

Table 3.5: Summary of the bias and 95% limits of agreement between mocap and OpenCap at discrete points for selected movements.

	Peak Knee Flexion	Peak Hip Flexion	Peak Ankle Dorsiflexion	Peak Hip Ab/Adduction	Peak Hip Rotation
Squat	-6.6° -11.5 to -1.7°	0.6° -10.1 to 11.2°	4.5° -2.6 to 11.6°	1.1° -6.3 to 8.5°	-6.2° -12.8 to 0.3°
SL Squat	-6.5° -14.9 to 1.8°	-12.5° -26.4 to 1.4°	8.4° 2.4 to 14.3°	2.3° -7.3 to 11.9°	7.2° -5.3 to 19.7°
Drop Vertical Jump	-2.6° -9.8 to 4.6°	-3.6 -11.1 to 4.0°	9.7° 3.7 to 15.6°	-1.0° -9.6 to 7.6°	-2.6° -7.1 to 2.0°
SL Drop Vertical Jump	-6.5° -14.1 to 1.1°	-5.9° -16.3 to 4.6°	9.5° -0.3 to 19.2°	-0.1° -8.6 to 8.5°	-1.9° -10.3 to 6.6°
Lunge and Twist	-11.1° -15.7 to -6.5°	-11.8° -20.1 to -3.5°	9.5° 2.8 to 16.1°	1.1° -16.7 to 18.9°	-0.5° -8.9 to 7.8°

Chapter 4 DISCUSSION

This study evaluated the accessibility and accuracy of a smartphone-based motion capture system against the current gold standard marker-based motion capture. In a qualitative comparison of accessibility between the two technologies, OpenCap had reduced time, cost, and expertise requirements to analyze human motion and was therefore more user-friendly. The system also required considerably less storage space and had few failed trials. The results captured across movements were then presented for lower extremity kinematics for nine exercise movements compared between OpenCap and gold standard mocap. Overall, accuracy varied across tasks and joints, and may be dependent on factors such as the speed of the movement, joint range of motion, and whether the task is single or dual limb. The analysis of discrete points showed there are the least systematic differences for hip flexion and more systematic differences for the remaining joint angles.

4.1 Usability

Data collection and processing was approximately 12 times faster for OpenCap. This is because setup does not involve instrumentation of subjects, and calibration is faster. Processing was also faster because kinematics were automatically estimated using cloud computing. The OpenCap system used in this study was approximately 400 times cheaper than the mocap system used in the study because it only includes smartphone cameras and tripods. Furthermore, OpenCap does not require a dedicated lab space and data can be collected anywhere with wifi. This decreased cost, data collection and processing time along with portability makes OpenCap a more accessible platform. This will allow for research studies with larger sample sizes to help elucidate more biomechanical markers associated with injury.

There were minimal challenges with trial failure for OpenCap (2% of trials), which operators should be aware of when collecting data. It is more apparent when mocap trials need to be recaptured to obtain three successful trials during data collection. For example, motion capture issues that warranted an immediate redo with an additional trial included force plate errors, markers falling off or covered markers resulting in large gaps in the marker trajectories. However, it was less apparent when OpenCap trials failed because it took time for the videos to be processed in the cloud and this did not always happen during data collection or the video data did process and looked usable in the cloud, but upon further analysis was unusable. However, collecting additional trials adds minimal time to data collection and would not increase data processing time because all the OpenCap kinematic data is processed automatically in the cloud. Furthermore, with additional algorithm training, this problem could be reduced.

The failed trials were also from different subjects and different tasks therefore suggesting there was not a setup issue with one subject or a systematic problem with OpenCap not being able to capture one movement type. However, most of the failed trials were from single limb tasks. This may be because it is more difficult for the OpenPose estimation algorithm to differentiate between limbs during single limb tasks, leading to crossing over of segments.

4.2 Accuracy

The accuracy of OpenCap's kinematics fall in the range reported in the literature for OpenCap validation (64) and other mobile movement assessment tools including IMUs, Theia3D, and Microsoft Kinect. Uhlrich *et al* reported 2.0 - 10.2° kinematic error across lower-extremity degrees of freedom for squat, drop vertical jump, gait, and sit to stand tasks (56,63,64). RMSE for Theia3D range from 2.6 - 11.2° for gait and 1.9 - 15.9° across twenty-

eight different movement tasks (cutting, step down, countermovement jump, squat, etc.) with the highest RMSEs for hip rotation (50,65). Errors reported for IMUs range from 2.0 - 12° across all lower-extremity angles for athletic tasks including single leg drop jump, double leg drop jump, cutting, single leg squat, and crossover (58,66,67). This suggests that OpenCap could be a suitable alternative to marker-based motion capture especially in cases where the practical benefits of smartphone markerless motion capture are necessary.

The movements collected with OpenCap setup two, lunge and twist and broad jump, required the subject to be further away from the cameras as compared to OpenCap setup one. Subjects were at a maximum approximate distance of six feet away from the center camera in OpenCap setup one. For single leg broad jump and lunge and twist, subjects started approximately 16 feet away from the center camera in OpenCap setup two. The extended distance of the subject from the camera may have affected the accuracy of OpenCap in setup two reflected in the larger RMSEs observed for these movements shown in Table 3.2, and sensitivity analysis of OpenCap accuracy based on distance is warranted.

The largest relative differences were observed in the transverse plane, hip rotation, where the percentage joint excursion RMSE ranged from 27% to 100%. However, these differences are challenging to interpret due to the likely presence of error from both systems and the lack of ground truth measurements. Larger between system differences during faster, jumping movements can also be explained by limitations from both systems. Marker errors induced by skin tissue artifacts are more apparent in faster movements [68]. Skin tissue artifacts describe the relative movement between surface markers and underlying bone. This phenomenon is both movement and subject dependent and may cause the most misrepresentation of internal/external and abduction/adduction movements (68). For example, it has been shown that skin mounted marker clusters move relative to the underlying bone during various tasks introducing errors up to 40mm at the thigh and 15mm at

the shank (69). Between system differences for faster movements could also be due to OpenCap parameters such as capture rate (60Hz) or challenges in differentiating segments with the OpenPose estimation algorithm. The smallest relative differences were observed for knee and hip flexion where the percentage joint excursion RMSE ranged from 6% to 17% and 5% to 19%, respectively. These joints undergo the largest ranges of motion for the movements presented here which may minimize between-system differences. In both cases, the smallest relative difference was for the squat suggesting higher accuracy in these joint angles for this task.

The magnitude of between-system differences was most apparent at the ankle with RMSEs ranging from 5.1 to 11.3° for all of the movements. This may be because of the machine learning algorithms, OpenPose and LSTM, used in the processing of video data to obtain joint kinematics. OpenPose, the key point detection algorithm, includes a specifically trained foot model, however the largest errors in key point identification are reported for the ankle in the original validation of the algorithm (67,68). After key points are identified, the neural network, LSTM, is used to augment the marker set. As previously mentioned, an arm and body model were trained to predict the position of markers, but no specific foot model. The majority of the training data for the LSTM model included walking and running (seven of the ten data sets) (66,67). The remaining three data sets included functional tasks such as cutting, double- and single-legged jump, squat, squat jump, and sit-to-stand. More data from a variety of tasks may overall help to improve the accuracy of OpenCap. Specifically, further training of the LSTM model is underway to improve the accuracy at the ankle and this should be evaluated in the future.

4.3 Generalized Linear Mixed Model

The generalized linear mixed model showed that for all movements, the factors that contributed the most variability to the response were joint, time, and the two-way interaction between technology and joint as shown in the Appendix. The significant effect of the two-way interaction between technology and joint suggests the differences between OpenCap and mocap depend on the joint for all the movements where there is a significant difference between the technologies. Most of the variance is due to these factors as joints are inherently different and undergo different ranges of motion and the joint angle value changes over the phase of the movement (time).

The model also showed that in most cases the differences between OpenCap and mocap depend on time as shown by the significant effect of the two-way interaction between technology and time, except for single leg squat. The replicate factor also significantly affected the response for all movements except the countermovement jump, single leg countermovement jump, and the lunge and twist. Both the two-way interaction between technology and time and the replicate factor did not contribute as large of a source of variability as the aforementioned fixed effects. Replicate could be further explored in the future to understand how the replicate number influences the response. For example, there may be a training effect resulting in a better quality second repetition of a movement than the first.

Furthermore, the model also showed there was not a significant effect of the two-way interaction between replicate and technology for all the movements, except heel touch, suggesting that in most cases, the differences between OpenCap and mocap do not depend on replicate. This makes sense because less variability is expected between replicates of each movement. Furthermore, the variation between replicates could be considered acceptable as humans inherently cannot do a movement the same exact way multiple times and in clinical

practice replicates are often averaged to account for this inherent variability. Therefore, the variability between technologies may be acceptable if it is less than or close to the magnitude of the variability for replicate as described by the sum of squares. Thus, the ratio of the sum of squares between technology and replicate suggests that the differences between technology may be acceptable for squat, single leg squat, countermovement jump, drop vertical jump, and single leg broad jump, but not acceptable for single leg countermovement jump, single leg drop vertical jump, heel touch, and lunge and twist. This ratio is the greatest for the lunge due to relatively low replicate variability, but relatively high technology variability suggesting that the differences in technology may be very important for this movement. The ratio is the smallest for the broad jump, however this may be due to the relatively large variability in replicates as subjects appear to execute this movement with low repeatability. This may suggest the broad jump is not an appropriate task to use for movement screening.

The significant effect of the three-way interaction of technology, joint and replicate for several of the movements suggests that in most cases the differences between technologies depend on multiple factors and all of the variability has not been accounted for. This is a limitation of the model. Furthermore, omitting the three-way interaction of technology time, and joint is a limitation and should be evaluated in the future using a more powerful statistical software package. This mixed effect model serves as a framework for future experimental design and studies that evaluate questions such as which joint is most variable or where in the movement cycle is there the most variation.

4.4 Differences across Movement Cycle

Squat, single leg squat, drop vertical jump, and single leg drop vertical jump were further analyzed as representative tasks. These tasks were chosen because they include a mix of single and double limb jumping and non-jumping. In all these movements, OpenCap

indicated more dorsiflexion in the ankle at each discrete point than mocap did as shown in Figure 3.3. Additionally, knee flexion was underestimated which was especially apparent in the squat and single leg squat. The squat challenges flexibility or range of motion as athletes were instructed to squat as deep as possible. The average total range of motion (joint excursion) for knee flexion for the squat pattern in the 10 subjects was 123° and ranged from 95 to 140°, whereas for all other movements, the average total knee joint excursion was less than 100°. Hip flexion was also underestimated in the tasks and most apparent for the single leg squat. During this motion, the thigh or the subject's hands on their hips may have partially or fully occluded the hip joint making it difficult for OpenPose to accurately track the position of the hip key points especially at deeper ranges of flexion. Similar reasons may have resulted in the larger differences seen for hip adduction in the single leg squat.

The between-system differences were less apparent for hip and knee flexion for the drop vertical jump and single leg drop vertical jump at greater joint excursion as compared to the squat and single leg squat, which may be because of decreased joint excursion during these jumping tasks. Furthermore, larger between-system differences were apparent at points of contact with the ground during the single leg drop vertical jump and the drop vertical jump. This may be because of skin tissue artifact with the marker-based system suggesting that OpenCap could be a better solution for dynamic movements where marker movement is an issue. OpenCap may be more problematic with motions that have a large joint excursion or single limb tasks as there may be less spatial differentiation of segments leading to differences. Accuracy and differences between OpenCap and mocap seem to vary across task and joint and may depend on features such as speed of task, joint excursion, single or dual limb, and distance from the cameras.

4.5 Discrete Points

Discrete peak points of selected movement tasks were evaluated in this study to determine the extent to which systematic or random differences between OpenCap and mocap could affect clinical interpretations or decision making. Peak points are used to assess movement quality, predict injury risk, or evaluate athletes returning to sport. The tasks considered most clinically relevant are included along with tasks where accuracy was the best and worst across the movement cycle for all joint angles as described in previous sections. Specifically, the squat was evaluated because it had the highest accuracy in the most joints (Table 3.2). To compare single limb and dual limb movements, the single limb squat was evaluated. The single limb squat also seemed to have larger between-system differences at greater joint excursions which was of interest. The lunge and twist was evaluated because it had the lowest accuracy in many of the joints (Table 3.2) and the difference plot (Appendix) seemed to show a consistent offset in the sagittal plane, which warranted further evaluation. The drop vertical jump and single leg drop vertical jump are clinically relevant movements and it was of interest to compare peak points in single limb vs dual limb jumping movements (68,69). Therefore, a more in-depth analysis of these movements is presented.

For all movements, there was a moderate to very strong correlation for peak knee flexion and peak hip flexion and moderate to strong correlation for peak ankle flexion between OpenCap and mocap, which was expected as generally motion capture is most accurate for sagittal plane motion. The correlations were lower for hip adduction especially for the lunge and twist, which could have been caused by occlusion of the hip by the thigh during this motion. There was a low to very strong correlation for peak hip rotation. The wide range suggests that peak hip rotation measures may be movement dependent and subject to previously mentioned challenges of capturing transverse plane motion. Pearson's correlation coefficient gives information about the strength of the relationship between two variables, but

it does assess the agreement. High correlation does not automatically imply good agreement and therefore the Bland Altman method was used to represent the data and assess the agreement.

The Bland Altman plots, Figure 3.3, show less variability within a subject's trials than between subjects, as demonstrated by the clustering between each set of colored dots. This indicates there is a greater level of repeatability within a subject and a session. The accessibility of OpenCap allows for frequent capture of athletes, however these repeated movement assessments are most informative if OpenCap is reliable and able to detect changes in athletes over time. Further inter-session repeatability analysis should be conducted in the future to bolster the reliability of OpenCap.

Figure 3.3 shows similar trends with certain subjects having lower or higher bias across all joint angles. For example, subject 8 (black) visually appears to have lower mean bias for peak hip flexion, knee flexion, hip rotation, and hip adduction for all movements whereas subject 7 (dark red) or subject 3 (cyan) appear to have a greater mean bias. This suggests that accuracy might be subject-dependent. Subject anthropometrics, anatomy, or even clothing could affect the accuracy of the OpenPose estimation algorithm, marker placement, skin tissue artifacts, and/or scaling of the model and therefore the kinematics (69,70). This is an important factor for consideration by researchers, coaches, and clinicians, when using motion capture technology as the assessment tool accuracy may vary with subjects.

The Bland Altman plots, Figure 3.3, show varying trends depending on the joint and the movement. Systematic differences include either fixed or proportional bias where fixed bias gives values that are higher or lower than those from the other method by a constant amount whereas proportional bias gives values that are higher or lower than those from the other method by an amount that is proportional to the magnitude of the measured value

(71,72). Fixed or proportional bias provides an opportunity to calculate the joint angle that mocap would have estimated when provided with OpenCap data whereas a bias with no trend does not.

For example, for the drop vertical jump movement, there appears to be a variable trend in bias for hip flexion, a fixed bias for ankle dorsiflexion, and a proportional bias for knee flexion, hip rotation, and hip abduction as shown in Figure 3.3C. More specifically, for peak hip flexion there appears to be a random scatter and no consistent trend. For ankle dorsiflexion, OpenCap appears to give values that are higher than mocap by a constant amount indicated by the consistent spread around the mean bias of 9.7°, suggesting a systematic fixed bias. Finally, for peak knee flexion, peak hip rotation, and peak hip abduction, the bias changes with increasing peak joint angle suggesting a systematic proportional bias. Similar patterns are observed for the single limb drop jump task suggesting that capture at peak points may be similar for jumping tasks.

Across all movements, the smallest mean bias is seen for hip adduction/abduction ranging from -0.1 to 2.3°. However, this joint also has the largest LOA and trends of the bias seem to vary depending on movement. For example, when adduction is observed, the bias is inconsistent for a single leg squat and proportional for the single leg drop vertical jump and the lunge and twist. A larger mean bias is observed for peak ankle dorsiflexion. However, this bias is approximately 9.5° for the drop vertical jump, single leg drop vertical jump, and lunge. This would suggest that there is a systematic offset of approximately 9.5° at peak ankle dorsiflexion for these movements. The largest variability in the mean bias is seen for hip flexion and hip rotation. The bias does not follow a trend in most cases for hip flexion, whereas it is proportional for hip rotation.

The mean bias for knee flexion is approximately -6.5° for squat, single leg squat, and single leg drop vertical jump and the LOA are within 6° for all the movements. This suggests

that knee flexion is primarily underestimated by OpenCap, however the bias does not appear to be a systematic fixed offset. There is a proportional offset for each movement, except the lunge and the direction of the trend is different between the jumping movements and the squatting movements. Furthermore, there appears to be a proportional bias for peak knee flexion for the squat until about 140°. At these extreme ranges of motion, the musculoskeletal model limits are reached, which suggests that model used may not be a good representation of the range of motion for collegiate athletes. Constrained models (i.e., models with limits on range of motion) help to increase accuracy but may not capture extreme ranges of motion for all tasks.

The evaluation of peak points with the Bland Altman method shows that OpenCap may have the most systematic offsets for peak knee flexion, ankle dorsiflexion, and hip rotation and the most random offsets for peak hip flexion and adduction when compared to marker-based motion capture. However, this small sample size makes it challenging to interpret the data; a larger n would help to increase the confidence in the data trends and decrease the LOAs. Despite this, the varying bias, LOAs, and trends for each movement suggests that OpenCap may be better at capturing some movements vs others, but broad conclusions cannot be drawn that pertain to all movements and joints.

Between-system differences were apparent across the movement cycle as seen in Figure 3.2. However, in cases where the differences were systematic, interchangeable use of OpenCap is still viable if clinicians are made aware of these consistent differences. Clinicians should be aware of this when deciding to use smartphone-based motion capture as an alternative to marker-based motion capture as the magnitude of bias and whether it is systematic or not may influence the conclusions that are drawn from a movement screen. For example, if a coach is screening athletes to determine if they can dual limb squat to at least 90° of knee flexion following an injury, OpenCap may be appropriate to use. OpenCap

underestimates knee flexion and this underestimation appears to be less at lower ranges of motion. At greater ranges of motion, the bias is greater, however this data suggests that OpenCap should still be able to indicate that 90° was achieved even with the underestimation. However, if the question is related to hip flexion for a drop vertical jump, such as does the athlete reach a peak hip flexion of at least 70° to evaluate risk of ACL injury, a coach may be less confident in OpenCap due to the varying trends seen in the Bland Altman plot. These factors should be taken into consideration for experimental design that seeks to evaluate if OpenCap is an appropriate tool for assessing movement.

4.6 Limitations

There are some limitations that affect the interpretation of the findings. First, the data presented is only from 10 subjects. This small sample size also results in the relatively large LOA observed in the Bland Altman plots. In addition, the sample size includes only healthy female collegiate athletes from ground-based sports. This sample size and relatively homogenous population may limit the generalizability of the results. Furthermore, mocap was considered the gold standard to compare OpenCap to; however, mocap has its own limitations including soft tissue artifacts and marker occlusion that affect the accuracy of the results.

The event identification process for this study for the beginning and end point of each movement was systematic, but manual, which may have resulted in more variability between trials. In the future, more repeatable and accurate methods should be used to identify these events to reduce the variability between trials. The lab space also constrained the OpenCap capture volume which created challenges collecting movements such as the lateral shuffle and cutting maneuver. However, up to five iPhones can be used in either a vertical or

horizontal orientation, which has the potential to drastically increase the capture volume. The limits of this would need to be tested.

4.7 Future Work

Some OpenCap trials were excluded from the analysis due to poor data quality resulting in only two trials for some movements and subjects. One reason for this poor data quality was the misidentification of landmarks and crossing over of limbs. For example, Figure 4.1, left shows the right limb being identified as the left limb. This occurred in multiple frames of the video and resulted in the knee angles shown in Figure 4.1 right. OpenCap supports a secondary pose estimation algorithm, HRNet (73). Further analysis should evaluate the ability of this pose estimation algorithm and the updated OpenPose estimation algorithm to correctly identify landmarks with no crossing over of segments. In addition, more than three trials should have been collected to ensure the three best trials could be selected for analysis.

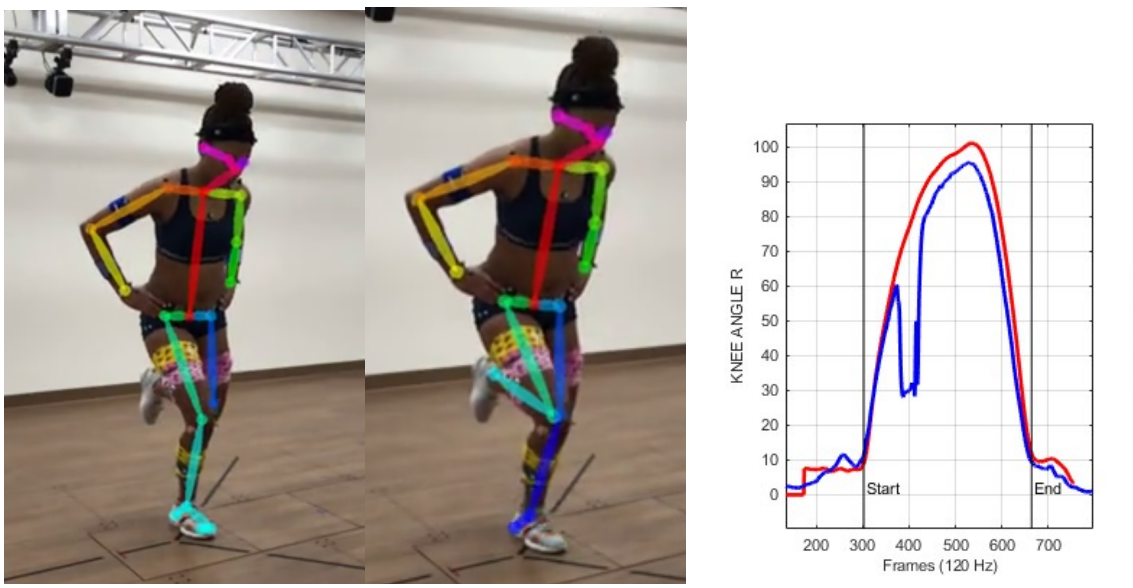

Figure 4.1: Subject completing a single leg squat. The colored keypoints on the left image correctly identify the left and right limbs. The right and left limbs are crossed over in the center image and result in the knee flexion plot shown on the right.

For each task, a longer movement cycle was evaluated than what is currently considered clinically relevant. Some features of these movements have yet to be associated with injury risk or return to play following injury. For example, to date, there has been no research correlating ankle plantar flexion angle during the jumping portion of the jumping tasks to injury risk or to evaluate return to sport. However, it is possible that movement features yet to be associated with injury are identified in this analysis, which is the reason for including the longer movement cycle. Furthermore, a longer movement cycle was included for the purpose of conducting principal component analysis (PCA) and clustering in future studies to identify patterns of motion in the dataset that explain the largest amount of variance. This analysis would help to determine the most important variables (e.g., kinematic features) that contribute to the observed movement patterns. These clusters could then be related to *a priori* ideas of injury mechanics. This analysis would also help to reveal redundancy in movement tasks; movement tasks that target the same constructs. Removing redundancy would help to form an optimal set of movement tasks that challenge all movement constructs.

Newer versions of OpenCap and Addbiomechanics have recently been released. OpenCap updates include changes to syncing and machine learning algorithms and updates to Addbiomechanics include changes to algorithms and fixing issues with estimation of ankle angles. Data analysis should be repeated to incorporate these updates and the remaining movements that were collected, but not included in this analysis. OpenCap estimated kinetics should then be evaluated as muscle dynamics may be more valuable in terms of injury prediction. For example, there may be more apparent differences in kinetics such as peak ground reaction force and knee extension moment in injured vs non-injured limbs and more research positively correlating joint moments to injury risk (73), however this was out of the scope of this work. An evaluation of OpenCap kinematics was critical before evaluating

kinetics because reliable joint kinetics depend on accurate kinematics and any inaccuracies in kinematics will propagate to even larger errors in joint kinetics (74).

Chapter 5 CONCLUSIONS

This project originated from the need for accessible and standardized measures of athletic movement. Evaluation of movement is important for identifying suboptimal movement that may increase athletes' risk of injury and identifying optimal movement strategies that may help to increase performance. OpenCap's affordability, quick implementation, accessibility to non-experts, and portability makes it suitable for widespread implementation across diverse athlete populations. We demonstrated that more detailed and objective data can be obtained with OpenCap as compared to a visual assessment, which may help highlight potential movement abnormalities in athletes that cannot be detected by the human eye. The analysis of the accuracy and between-system agreement lent insight into which type of movements this platform may be most applicable for and where between-system differences arise. The generalized linear mixed model helped identify movement tasks where the variability between technologies may be acceptable. This work is a foundation for future studies to evaluate OpenCap for more specific clinical questions to better understand the underlying mechanisms contributing to specific injuries.

Chapter 6 REFERENCES

1. Lu T-W, Chang C-F. Biomechanics of human movement and its clinical applications. Kaohsiung J Med Sci. 2012 Feb;28(2 Suppl):S13-25.

2. Cook G, Burton L, Hoogenboom B. Pre-participation screening: the use of fundamental movements as an assessment of function - part 1. N Am J Sports Phys Ther. 2006 May;1(2):62–72.

3. Kritz M, Cronin J, Hume P. The Bodyweight Squat: A Movement Screen for the Squat Pattern. Strength & Conditioning Journal. 2009 Feb;31(1):76.

4. López-Nava IH, Muñoz-Meléndez A. Wearable Inertial Sensors for Human Motion Analysis: A Review. IEEE Sens J. 2016 Nov;16(22):7821–34.

5. Islam R, Bennasar M, Nicholas K, Button K, Holland S, Mulholland P, Price B, Al-Amri M. A Nonproprietary Movement Analysis System (MoJoXlab) Based on Wearable Inertial Measurement Units Applicable to Healthy Participants and Those With Anterior Cruciate Ligament Reconstruction Across a Range of Complex Tasks: Validation Study. JMIR Mhealth Uhealth. 2020 Jun 16;8(6):e17872.

6. Herman T, Giladi N, Hausdorff JM. Properties of the "timed up and go" test: more than meets the eye. Gerontology. 2011;57(3):203–10.

7. Guyatt GH, Sullivan MJ, Thompson PJ, Fallen EL, Pugsley SO, Taylor DW, Berman LB. The 6-minute walk: a new measure of exercise capacity in patients with chronic heart failure. Can Med Assoc J. 1985 Apr 15;132(8):919–23.

8. Podsiadlo D, Richardson S. The timed "Up & Go": a test of basic functional mobility for frail elderly persons. J Am Geriatr Soc. 1991 Feb;39(2):142–8.

9. Baker R. The history of gait analysis before the advent of modern computers. Gait Posture. 2007 Sep;26(3):331–42.

10. Sutherland DH, Hagy JL. Measurement of gait movements from motion picture film. J Bone Joint Surg Am. 1972 Jun;54(4):787–97.

11. Hendricks RM, Khasawneh MT. An Investigation into the Use and Meaning of Parkinson's Disease Clinical Scale Scores [Internet]. Vol. 2021, Parkinson's Disease. 2021. p. 1–7. Available from: http://dx.doi.org/10.1155/2021/1765220

12. Cook G, Burton L, Hoogenboom BJ, Voight M. Functional movement screening: the use of fundamental movements as an assessment of function - part 1. Int J Sports Phys Ther. 2014 May;9(3):396–409.

13. Chorba RS, Chorba DJ, Bouillon LE, Overmyer CA, Landis JA. Use of a functional movement screening tool to determine injury risk in female collegiate athletes. N Am J Sports Phys Ther. 2010 Jun;5(2):47–54.

14. Frost DM, Beach TAC, Callaghan JP, McGill SM. Using the Functional Movement

Screen™ to evaluate the effectiveness of training. J Strength Cond Res. 2012 Jun;26(6):1620–30.

15. Chimera NJ, Warren M. Use of clinical movement screening tests to predict injury in sport. World J Orthop. 2016 Apr 18;7(4):202–17.

16. Lally EM, Ericksen H, Earl-Boehm J. Measurement Properties of Clinically Accessible Movement Assessment Tools for Analyzing Single-Leg Squats and Step-Downs: A Systematic Review. J Sport Rehabil. 2022 May 1;31(4):476–89.

17. Bennett H, Davison K, Arnold J, Slattery F, Martin M, Norton K. Multicomponent Musculoskeletal Movement Assessment Tools: A Systematic Review and Critical Appraisal of Their Development and Applicability to Professional Practice. J Strength Cond Res. 2017 Oct;31(10):2903–19.

18. McGuigan MR, Winchester JB. The relationship between isometric and dynamic strength in college football players. J Sports Sci Med. 2008 Mar 1;7(1):101–5.

19. Mandic R, Jakovljevic S, Jaric S. Effects of countermovement depth on kinematic and kinetic patterns of maximum vertical jumps. J Electromyogr Kinesiol. 2015 Apr;25(2):265–72.

20. Tan T, Gatti AA, Fan B, Shea KG, Sherman SL, Uhlrich SD, Hicks JL, Delp SL, Shull PB, Chaudhari AS. A scoping review of portable sensing for out-of-lab anterior cruciate ligament injury prevention and rehabilitation. NPJ Digit Med. 2023 Mar 18;6(1):46.

21. Hewett TE, Myer GD, Ford KR, Heidt RS Jr, Colosimo AJ, McLean SG, van den Bogert AJ, Paterno MV, Succop P. Biomechanical measures of neuromuscular control and valgus loading of the knee predict anterior cruciate ligament injury risk in female athletes: a prospective study. Am J Sports Med. 2005 Apr;33(4):492–501.

22. Kotsifaki A, Van Rossom S, Whiteley R, Korakakis V, Bahr R, Sideris V, Jonkers I. Single leg vertical jump performance identifies knee function deficits at return to sport after ACL reconstruction in male athletes. Br J Sports Med. 2022 May 1;56(9):490–8.

23. Leppänen M, Pasanen K, Kujala UM, Vasankari T, Kannus P, Äyrämö S, Krosshaug T, Bahr R, Avela J, Pertunnen J, Parkakari J. Stiff Landings Are Associated With Increased ACL Injury Risk in Young Female Basketball and Floorball Players. Am J Sports Med. 2017 Feb;45(2):386–93.

24. Hughes G, Musco P, Caine S, Howe L. Lower Limb Asymmetry After Anterior Cruciate Ligament Reconstruction in Adolescent Athletes: A Systematic Review and Meta-Analysis. J Athl Train. 2020 Aug 1;55(8):811–25.

25. Decker MJ, Torry MR, Wyland DJ, Sterett WI, Richard Steadman J. Gender differences in lower extremity kinematics, kinetics and energy absorption during landing. Clin Biomech . 2003 Aug;18(7):662–9.

26. Fox AS, Bonacci J, McLean SG, Spittle M, Saunders N. What is normal? Female lower limb kinematic profiles during athletic tasks used to examine anterior cruciate ligament injury risk: a systematic review. Sports Med. 2014 Jun;44(6):815–32.

27. Pollard CD, Sigward SM, Powers CM. Limited hip and knee flexion during landing is associated with increased frontal plane knee motion and moments. Clin Biomech . 2010 Feb;25(2):142–6.

28. Powers CM. The influence of altered lower-extremity kinematics on patellofemoral joint dysfunction: a theoretical perspective. J Orthop Sports Phys Ther. 2003 Nov;33(11):639–46.

29. Lepley AS, Kuenze CM. Hip and Knee Kinematics and Kinetics During Landing Tasks After Anterior Cruciate Ligament Reconstruction: A Systematic Review and Meta-Analysis. J Athl Train. 2018 Feb;53(2):144–59.

30. Yamazaki J, Muneta T, Ju YJ, Sekiya I. Differences in kinematics of single leg squatting between anterior cruciate ligament-injured patients and healthy controls. Knee Surg Sports Traumatol Arthrosc. 2010 Jan;18(1):56–63.

31. Yamazaki J, Muneta T, Ju Y-J, Koga H, Morito T, Sekiya I. The kinematic analysis of female subjects after double-bundle anterior cruciate ligament reconstruction during single-leg squatting. J Orthop Sci. 2013 Mar;18(2):284–9.

32. DeHaven KE, Lintner DM. Athletic injuries: comparison by age, sport, and gender. Am J Sports Med. 1986 May-Jun;14(3):218–24.

33. Boling MC, Padua DA, Marshall SW, Guskiewicz K, Pyne S, Beutler A. A prospective investigation of biomechanical risk factors for patellofemoral pain syndrome: the Joint Undertaking to Monitor and Prevent ACL Injury (JUMP-ACL) cohort. Am J Sports Med. 2009 Nov;37(11):2108–16.

34. Souza RB, Powers CM. Differences in hip kinematics, muscle strength, and muscle activation between subjects with and without patellofemoral pain. J Orthop Sports Phys Ther. 2009 Jan;39(1):12–9.

35. Nakagawa TH, Moriya ETU, Maciel CD, Serrão FV. Trunk, pelvis, hip, and knee kinematics, hip strength, and gluteal muscle activation during a single-leg squat in males and females with and without patellofemoral pain syndrome. J Orthop Sports Phys Ther. 2012 Jun;42(6):491–501.

36. Whittaker JL, Woodhouse LJ, Nettel-Aguirre A, Emery CA. Outcomes associated with early post-traumatic osteoarthritis and other negative health consequences 3-10 years following knee joint injury in youth sport. Osteoarthritis Cartilage. 2015 Jul;23(7):1122–9.

37. Noyes FR, Barber-Westin SD, Fleckenstein C, Walsh C, West J. The drop-jump screening test: difference in lower limb control by gender and effect of neuromuscular training in female athletes. Am J Sports Med. 2005 Feb;33(2):197–207.

38. Kritz M. Development, reliability and effectiveness of the Movement Competency Screen (MCS).

39. Kraus K, Schutz E, Taylor WR, Doyscher R. EFFICACY OF THE FUNCTIONAL MOVEMENT SCREEN: AREVIEW. Journal of Strength and Conditioning Research [Internet]. 2014 Dec; Available from: http://journals.lww.com/nsca-jscr

40. Zhao X, Ross G, Dowling B, Graham RB. Three-Dimensional Motion Capture Data of a Movement Screen from 183 Athletes. Sci Data. 2023 Apr 24;10(1):235.

41. Moran RW, Schneiders AG, Mason J, Sullivan SJ. Do Functional Movement Screen (FMS) composite scores predict subsequent injury? A systematic review with meta-analysis. Br J Sports Med. 2017 Dec;51(23):1661–9.

42. Weygers I, Kok M, Konings M, Hallez H, De Vroey H, Claeys K. Inertial Sensor-Based Lower Limb Joint Kinematics: A Methodological Systematic Review. Sensors [Internet]. 2020 Jan 26;20(3). Available from: http://dx.doi.org/10.3390/s20030673

43. Uhlrich SD, Falisse A, Kidziński Ł, Muccini J, Ko M, Chaudhari AS, Hicks JL, Delp SL. OpenCap: 3D human movement dynamics from smartphone videos [Internet]. bioRxiv. 2022 [cited 2022 Jul 12]. p. 2022.07.07.499061. Available from: https://www.biorxiv.org/content/10.1101/2022.07.07.499061v1

44. Camomilla V, Cappozzo A, Vannozzi G. Three-dimensional reconstruction of the human skeleton in motion. Handbook of human motion. 2018;17–45.

45. Slade P, Habib A, Hicks JL, Delp SL. An Open-Source and Wearable System for Measuring 3D Human Motion in Real-Time. IEEE Trans Biomed Eng. 2022 Feb;69(2):678–88.

46. Al Borno M, O'Day J, Ibarra V, Dunne J, Seth A, Habib A, Ong C, Hicks J, Uhlrich S, Delp S. OpenSense: An open-source toolbox for inertial-measurement-unit-based measurement of lower extremity kinematics over long durations. J Neuroeng Rehabil. 2022 Feb 20;19(1):22.

47. Clark RA, Pua Y-H, Fortin K, Ritchie C, Webster KE, Denehy L, Bryant AL. Validity of the Microsoft Kinect for assessment of postural control. Gait Posture. 2012 Jul;36(3):372–7.

48. Galna B, Barry G, Jackson D, Mhiripiri D, Olivier P, Rochester L. Accuracy of the Microsoft Kinect sensor for measuring movement in people with Parkinson's disease. Gait Posture. 2014 Apr;39(4):1062–8.

49. O'Reilly M, Caulfield B, Ward T, Johnston W, Doherty C. Wearable Inertial Sensor Systems for Lower Limb Exercise Detection and Evaluation: A Systematic Review. Sports Med. 2018 May;48(5):1221–46.

50. Kanko RM, Laende EK, Davis EM, Selbie WS, Deluzio KJ. Concurrent assessment of gait kinematics using marker-based and markerless motion capture. J Biomech. 2021 Oct 11;127:110665.

51. Kanko RM, Laende EK, Strutzenberger G, Brown M, Selbie WS, DePaul V, Scott SH, Deluzio KJ. Assessment of spatiotemporal gait parameters using a deep learning algorithm-based markerless motion capture system. J Biomech. 2021 Jun 9;122:110414.

52. Werling K, Raitor M, Stingel J, Hicks JL, Collins S, Delp SL, Karen Liu C. Rapid bilevel optimization to concurrently solve musculoskeletal scaling, marker registration, and inverse kinematic problems for human motion reconstruction [Internet]. bioRxiv. 2022 [cited 2023 Mar 15]. p. 2022.08.22.504896. Available from:

https://www.biorxiv.org/content/10.1101/2022.08.22.504896v1

53. Leboeuf F, Baker R, Barré A, Reay J, Jones R, Sangeux M. The conventional gait model, an open-source implementation that reproduces the past but prepares for the future. Gait Posture. 2019 Mar;69:235–41.

54. Schreven S, Beek PJ, Smeets JBJ. Optimising filtering parameters for a 3D motion analysis system. J Electromyogr Kinesiol. 2015 Oct 1;25(5):808–14.

55. Cao Z, Hidalgo G, Simon T, Wei S-E, Sheikh Y. OpenPose: Realtime Multi-Person 2D Pose Estimation Using Part Affinity Fields [Internet]. Vol. 43, IEEE Transactions on Pattern Analysis and Machine Intelligence. 2021. p. 172–86. Available from: http://dx.doi.org/10.1109/tpami.2019.2929257

56. opencap-core: Main OpenCap processing pipeline [Internet]. Github; [cited 2023 May 2]. Available from: https://github.com/stanfordnmbl/opencap-core

57. Lai AKM, Arnold AS, Wakeling JM. Why are Antagonist Muscles Co-activated in My Simulation? A Musculoskeletal Model for Analysing Human Locomotor Tasks. Ann Biomed Eng. 2017 Dec;45(12):2762–74.

58. Chia L, Andersen JT, McKay MJ, Sullivan J, Megalaa T, Pappas E. Evaluating the validity and reliability of inertial measurement units for determining knee and trunk kinematics during athletic landing and cutting movements. J Electromyogr Kinesiol. 2021 Oct;60:102589.

59. Schober P, Boer C, Schwarte LA. Correlation Coefficients: Appropriate Use and Interpretation. Anesth Analg. 2018 May;126(5):1763–8.

60. Bland JM, Altman DG. Statistical methods for assessing agreement between two methods of clinical measurement. Lancet. 1986 Feb 8;1(8476):307–10.

61. Macrum E, Bell DR, Boling M, Lewek M, Padua D. Effect of limiting ankle-dorsiflexion range of motion on lower extremity kinematics and muscle-activation patterns during a squat. J Sport Rehabil. 2012 May;21(2):144–50.

62. Wren TAL, Mueske NM, Brophy CH, Pace JL, Katzel MJ, Edison BR, Vandenberg CD, Zaslow TL. Hop Distance Symmetry Does Not Indicate Normal Landing Biomechanics in Adolescent Athletes With Recent Anterior Cruciate Ligament Reconstruction. J Orthop Sports Phys Ther. 2018 Aug;48(8):622–9.

63. Comfort P, Jones PA, Smith LC, Herrington L. Joint Kinetics and Kinematics During Common Lower Limb Rehabilitation Exercises. J Athl Train. 2015 Oct;50(10):1011–8.

64. Giavarina D. Understanding Bland Altman analysis. Biochem Med . 2015 Jun 5;25(2):141–51.

65. Song K, Hullfish TJ, Silva RS, Silbernagel KG, Baxter JR. Markerless motion capture estimates of lower extremity kinematics and kinetics are comparable to marker-based across 8 movements. bioRxiv [Internet]. 2023 Feb 22; Available from: http://dx.doi.org/10.1101/2023.02.21.526496

66. Fan B, Xia H, Xu J, Li Q, Shull PB. IMU-based knee flexion, abduction and internal rotation estimation during drop landing and cutting tasks. J Biomech. 2021 Jul 19;124:110549.

67. Dahl KD, Dunford KM, Wilson SA, Turnbull TL, Tashman S. Wearable sensor validation of sports-related movements for the lower extremity and trunk. Med Eng Phys. 2020 Oct;84:144–50.

68. Andersen MS, Benoit DL, Damsgaard M, Ramsey DK, Rasmussen J. Do kinematic models reduce the effects of soft tissue artefacts in skin marker-based motion analysis? An in vivo study of knee kinematics. J Biomech. 2010 Jan 19;43(2):268–73.

69. Benoit DL, Damsgaard M, Andersen MS. Surface marker cluster translation, rotation, scaling and deformation: Their contribution to soft tissue artefact and impact on knee joint kinematics. J Biomech. 2015 Jul 16;48(10):2124–9.

70. Ito N, Sigurðsson HB, Seymore KD, Arhos EK, Buchanan TS, Snyder-Mackler L, Silbernagel KG. Markerless motion capture: What clinician-scientists need to know right now. JSAMS Plus [Internet]. 2022 Oct;1. Available from: http://dx.doi.org/10.1016/j.jsampl.2022.100001

71. Liao JJZ, Capen R. An Improved Bland-Altman Method for Concordance Assessment. Int J Biostat [Internet]. 2011 Jan 6 [cited 2023 Apr 27];7(1). Available from: https://www.degruyter.com/document/doi/10.2202/1557-4679.1295/html

72. Ludbrook J. Confidence in Altman-Bland plots: a critical review of the method of differences. Clin Exp Pharmacol Physiol. 2010 Feb;37(2):143–9.

73. Sun K, Xiao B, Liu D, Wang J. Deep high-resolution representation learning for human pose estimation. In: 2019 IEEE/CVF Conference on Computer Vision and Pattern Recognition (CVPR). IEEE; 2019. p. 5693–703.

74. Colyer SL, Evans M, Cosker DP, Salo AIT. A Review of the Evolution of Vision-Based Motion Analysis and the Integration of Advanced Computer Vision Methods Towards Developing a Markerless System [Internet]. Vol. 4, Sports Medicine - Open. 2018. Available from: http://dx.doi.org/10.1186/s40798-018-0139-y

75. Bates NA, Ford KR, Myer GD, Hewett TE. Timing differences in the generation of ground reaction forces between the initial and secondary landing phases of the drop vertical jump. Clin Biomech . 2013 Aug;28(7):796–9.

76. Orishimo KF, Kremenic IJ, Mullaney MJ, McHugh MP, Nicholas SJ. Adaptations in single-leg hop biomechanics following anterior cruciate ligament reconstruction. Knee Surg Sports Traumatol Arthrosc. 2010 Nov;18(11):1587–93.

77. Farrokhi S, Pollard CD, Souza RB, Chen Y-J, Reischl S, Powers CM. Trunk position influences the kinematics, kinetics, and muscle activity of the lead lower extremity during the forward lunge exercise. J Orthop Sports Phys Ther. 2008 Jul;38(7):403–9.

Chapter 7 APPENDIX

7.1 Event Identification

For the squat, the start of the movement was defined as the largest increase in slope of either the right or left (whichever occurred first) knee flexion just before the subject began the ascent phase of the squat. This change in slope was approximated by an inflection point on the acceleration graph. The end of movement was defined as the largest decrease in slope of either the right or left (whichever occurred last) knee flexion approaching 0 degrees at the end of the descent phase. This change in slope was also approximated by an inflection point on the acceleration graph. The same approach was used for single leg squat, however the slope change of the leg of interest was used (e.g., right knee flexion for a right single leg squat). For heel touch, the start of the movement was also defined as the largest increase in slope of knee flexion of the limb that remained on the box. The end of movement was defined as the point at which contact with the force plate terminated.

For countermovement jump and single leg countermovement jump, the angular velocity of PELS marker, located superior to the posterior superior iliac spines, was used to identify the start and stop cycle. This marker was used as a surrogate to the center of mass (COM) as it is located at a similar height. The start of the movement cycle was defined as when the angular velocity of the PELS marker crossed the z axis indicating a directional change in the motion of the subject. The end of the movement was defined as when the PELS marker crossed the z axis following landing indicating the subject was beginning the return back to standing. For drop vertical jump and single leg drop vertical jump, the start of the movement was defined as the point of initial contact with the force plates of the left or right foot (whichever occurred first). Initial contact was defined as the first point the vertical ground reaction force exceeded 10 N (75). The end of the movement was defined as the PELS angular velocity crossing the z axis following the second landing signaling the end of the impact phase of landing.

For the broad jump, the start of the movement was defined as the largest increase in slope of knee flexion before ascent. The PELS marker was then used as an approximation for the subject's COM. The end of the movement was defined as the minimum vertical position of the PELS marker following impact which indicated the lowest point of the COM (76). For lunge and twist, the start of the movement was defined as the point of initial contact with the force plate of the leading leg. The end of movement was defined as the point contact with the force plate terminated (e.g., toe off) (77).

For a 45-degree cut, the start of the movement was defined as the point of initial contact with the force plate of the leg of interest to the point at which contact with the force plate terminated. The deceleration and lateral shuffle movements were broken up into three sections as the subjects completed the movement three consecutive times. The start of each was defined as the point of initial contact of the leg of interest and the end of each was the point at which contact with the force plate terminated. For Y Balance Test, the start of movement was defined when the PELS marker crossed the z axis into negative before the first reach direction (forward) and the end of the movement was defined as the point after the angular velocity of the PELS marker crossed the z axis into positive following the final reach (posteromedially).

7.2 Generalized Linear Mixed Model Results

The results from the generalized linear mixed model for each movement task are described in Figure 7.1.

Figure 7.1: Results from the generalized linear mixed model for each movement. The F value indicates the variability contributed by the factor. The covariance parameter estimates describe the variation due to the random effect of the subject and the residual is the variation that is not accounted for by the fixed and random effects in the model.

Squat

Type III Tests of Fixed Effects				
Effect	Num DF	Den DF	F Value	Pr > F
Technology	1	59031	145.49	<.0001
Time	100	59031	5016.85	<.0001
Joint	9	59031	177666	<.0001
Replicate	2	59031	86.46	<.0001
Technology*Time	100	59031	2.08	<.0001
Technology*Joint	9	59031	590.57	<.0001
Technology*Replicate	2	59031	0.43	0.6492
Time*Replicate	200	59031	6.88	<.0001
Joint*Time	900	59031	482.25	<.0001
Joint*Replicate	18	59031	22.86	<.0001
Technol*Time*Replica	200	59031	0.07	1.0000
Techno*Joint*Replica	18	59031	0.89	0.5867

Covariance Parameter Estimates		
Cov Parm	Estimate	Standard Error
Subject	8.4889	4.0049
Residual	40.5927	0.2363

Single Leg Squat

Type III Tests of Fixed Effects				
Effect	Num DF	Den DF	F Value	Pr > F
Technology	1	53981	125.45	<.0001
Time	100	53981	1672.12	<.0001
Joint	9	53981	70967.4	<.0001
Replicate	2	53981	79.25	<.0001
Technology*Time	100	53981	0.37	1.0000
Technology*Joint	9	53981	1106.63	<.0001
Technology*Replicate	2	53981	1.73	0.1764
Time*Replicate	200	53981	1.52	<.0001
Joint*Time	900	53981	149.30	<.0001
Joint*Replicate	18	53981	45.12	<.0001
Technol*Time*Replica	200	53981	0.07	1.0000
Techno*Joint*Replica	18	53981	1.98	0.0077

Covariance Parameter Estimates		
Cov Parm	Estimate	Standard Error
Subject	5.4468	2.5732
Residual	41.9572	0.2554

Counter-movement Jump

Type III Tests of Fixed Effects				
Effect	Num DF	Den DF	F Value	Pr > F
Technology	1	57011	1.15	0.2841
Time	100	57011	1174.25	<.0001
Joint	9	57011	24835.2	<.0001
Replicate	2	57011	1.74	0.1751
Technology*Time	100	57011	1.70	<.0001
Technology*Joint	9	57011	278.68	<.0001
Technology*Replicate	2	57011	0.08	0.9246
Time*Replicate	200	57011	1.25	0.0095
Joint*Time	900	57011	87.23	<.0001
Joint*Replicate	18	57011	1.84	0.0158
Technol*Time*Replica	200	57011	0.05	1.0000
Techno*Joint*Replica	18	57011	0.82	0.6760

Covariance Parameter Estimates		
Cov Parm	Estimate	Standard Error
Subject	8.0677	3.8167
Residual	151.65	0.8982

Figure 7.1, Continued

Single Leg Counter-movement Jump

Type III Tests of Fixed Effects				
Effect	Num DF	Den DF	F Value	Pr > F
Technology	1	58021	39.57	<.0001
Time	100	58021	1112.72	<.0001
Joint	9	58021	27519.9	<.0001
Replicate	2	58021	2.28	0.1028
Technology*Time	100	58021	6.01	<.0001
Technology*Joint	9	58021	530.09	<.0001
Technology*Replicate	2	58021	0.58	0.5613
Joint*Time	900	58021	51.89	<.0001
Time*Replicate	200	58021	1.50	<.0001
Joint*Replicate	18	58021	4.84	<.0001
Techno*Joint*Replica	18	58021	0.61	0.8949
Technol*Time*Replica	200	58021	0.06	1.0000

Covariance Parameter Estimates		
Cov Parm	Estimate	Standard Error
Subject	4.7813	2.2614
Residual	91.2256	0.5356

Drop Vertical Jump

Type III Tests of Fixed Effects				
Effect	Num DF	Den DF	F Value	Pr > F
Technology	1	59031	36.04	<.0001
Time	100	59031	2118.58	<.0001
Joint	9	59031	40876.6	<.0001
Replicate	2	59031	45.04	<.0001
Technology*Time	100	59031	4.07	<.0001
Technology*Joint	9	59031	389.79	<.0001
Technology*Replicate	2	59031	1.53	0.2169
Time*Replicate	200	59031	3.14	<.0001
Joint*Time	900	59031	132.26	<.0001
Joint*Replicate	18	59031	7.66	<.0001
Technol*Time*Replica	200	59031	0.07	1.0000
Techno*Joint*Replica	18	59031	0.27	0.9990

Covariance Parameter Estimates		
Cov Parm	Estimate	Standard Error
Subject	16.6628	7.8624
Residual	96.1832	0.5599

Single Leg Drop Vertical Jump

Type III Tests of Fixed Effects				
Effect	Num DF	Den DF	F Value	Pr > F
Technology	1	57011	43.60	<.0001
Time	100	57011	1216.88	<.0001
Joint	9	57011	30235.1	<.0001
Replicate	2	57011	3.94	0.0194
Technology*Time	100	57011	3.55	<.0001
Technology*Joint	9	57011	489.76	<.0001
Technology*Replicate	2	57011	0.22	0.8010
Time*Replicate	200	57011	0.79	0.9865
Joint*Time	900	57011	47.89	<.0001
Joint*Replicate	18	57011	9.86	<.0001
Technol*Time*Replica	200	57011	0.11	1.0000
Techno*Joint*Replica	18	57011	2.80	<.0001

Covariance Parameter Estimates		
Cov Parm	Estimate	Standard Error
Subject	21.4823	10.1376
Residual	85.6663	0.5074

Figure 7.1, Continued

Heel Touch

Type III Tests of Fixed Effects				
Effect	Num DF	Den DF	F Value	Pr > F
Technology	1	59031	1420.75	<.0001
Time	100	59031	1870.00	<.0001
Joint	9	59031	80089.1	<.0001
Replicate	2	59031	25.94	<.0001
Technology*Time	100	59031	25.10	<.0001
Technology*Joint	9	59031	2180.32	<.0001
Technology*Replicate	2	59031	6.07	0.0023
Time*Replicate	200	59031	0.18	1.0000
Joint*Time	900	59031	144.58	<.0001
Joint*Replicate	18	59031	25.92	<.0001
Technol*Time*Replica	200	59031	0.09	1.0000
Techno*Joint*Replica	18	59031	3.62	<.0001

Covariance Parameter Estimates		
Cov Parm	Estimate	Standard Error
Subject	1.5981	0.7557
Residual	29.9212	0.1742

Lunge and Twist

Type III Tests of Fixed Effects				
Effect	Num DF	Den DF	F Value	Pr > F
Technology	1	59031	950.61	<.0001
Time	100	59031	1246.14	<.0001
Joint	9	59031	185967	<.0001
Replicate	2	59031	1.85	0.1572
Technology*Time	100	59031	4.43	<.0001
Technology*Joint	9	59031	2385.72	<.0001
Technology*Replicate	2	59031	0.18	0.8360
Time*Replicate	200	59031	0.39	1.0000
Joint*Time	900	59031	106.05	<.0001
Joint*Replicate	18	59031	14.25	<.0001
Technol*Time*Replica	200	59031	0.05	1.0000
Techno*Joint*Replica	18	59031	5.28	<.0001

Covariance Parameter Estimates		
Cov Parm	Estimate	Standard Error
Subject	2.9823	1.4092
Residual	42.7351	0.2487

Figure 7.1, Continued

Single Leg Broad Jump

Type III Tests of Fixed Effects				
Effect	Num DF	Den DF	F Value	Pr > F
Technology	1	59031	1.80	0.1802
Time	100	59031	400.74	<.0001
Joint	9	59031	18974.5	<.0001
Replicate	2	59031	11.75	<.0001
Technology*Time	100	59031	3.75	<.0001
Technology*Joint	9	59031	87.07	<.0001
Technology*Replicate	2	59031	1.54	0.2151
Time*Replicate	200	59031	0.50	1.0000
Joint*Time	900	59031	35.02	<.0001
Joint*Replicate	18	59031	8.35	<.0001
Technol*Time*Replica	200	59031	0.10	1.0000
Techno*Joint*Replica	18	59031	1.49	0.0830

Covariance Parameter Estimates		
Cov Parm	Estimate	Standard Error
Subject	10.6122	5.0119
Residual	119.43	0.6952

7.3 Analysis of Missing Trials

Some of the movements included subjects with two replicates instead of three replicates due to failed trials identified during data analysis. To justify this, a subset of these movements was re-run all with two replicates instead of a mixture of two and three replicates to see if the results changed. Shown below (Table 7.1) is a summary of the Pearson correlation coefficient and Bland Altman parameters between the two methods for a left drop vertical jump as a representative task. Two subjects for the left drop vertical jump included only two replicates instead of three.

Table 7.1: Summary of the Pearson Correlation coefficients and Bland Altman parameters for the left drop vertical jump for all trials which includes two out of 10 subjects with two replicates compared to only two replicates from each of the 10 subjects.

	Knee flexion	Hip flexion	Ankle flexion	Hip adduction	Hip rotation
All trials	r = 0.94 Bias: -7.6° LOA: -0.4 to -14.8°	r = 0.95 Bias: -4.9° LOA: -14.9 to 5.1°	r = 0.66 Bias: 6.4° LOA: -2.5 to 15.3°	r = 0.65 Bias: 1.3° LOA: -9.7 to 12.4°	r = 0.65 Bias: -2.0° LOA: -18.3 to 14.3°
Two replicates per subject	r = 0.94 Bias: -8.3° LOA: -15.5 to -1.1°	r = 0.95 Bias: -6.5° LOA: -16.7 to 3.7°	r = 0.59 Bias: 6.2° LOA: -3.8 to 16.2	r = 0.65 Bias: 1.9° LOA: -9.7 to 13.6°	r = 0.65 Bias: -2.3° LOA: -19.7 to 15°

The Pearson correlation coefficients for each joint angle have the same classification regardless of if the two or three replicates were included for the analysis. Peak knee flexion and hip flexion are very strongly correlated, ankle flexion, hip adduction, and hip rotation are moderately correlated. The Bland Altman plots show similar trends in the data and the parameters shown in the table are similar.

7.4 Between-system Differences Across Each Movement Task

The mean ± SD for hip flexion, hip abduction/adduction, hip rotation, knee flexion, and ankle flexion across each movement task and the mean ± SD of the between-system differences across each joint angle of each movement task are shown in Figure 7.2. Positive indicates hip adduction and negative indicates hip abduction. Positive indicates internal rotation and negative indicates external rotation.

Figure 7.2: Mean ± SD waveforms (n=10 subjects) from mocap (blue), and OpenCap (red) for hip flexion, hip abduction/adduction, hip rotation, knee flexion, and ankle flexion across the movement cycle of each movement task. The black line with shading indicates the mean ± SD between-system difference across the cycle of the movement.

Squat

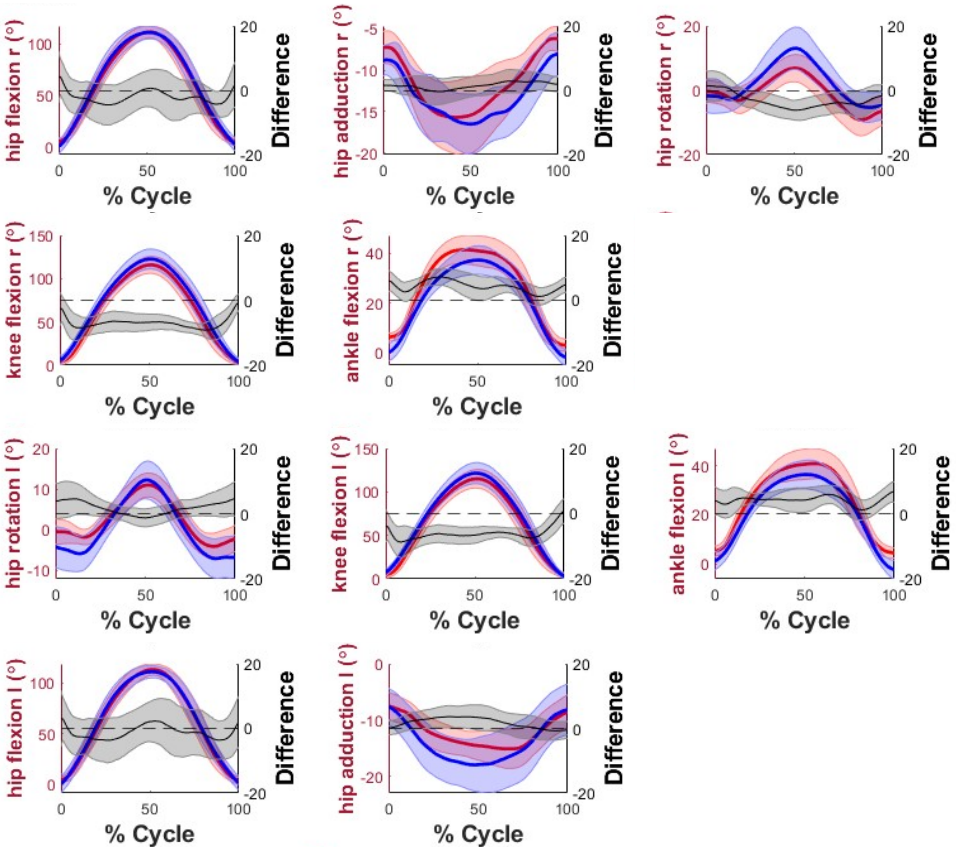

Single Leg Squat

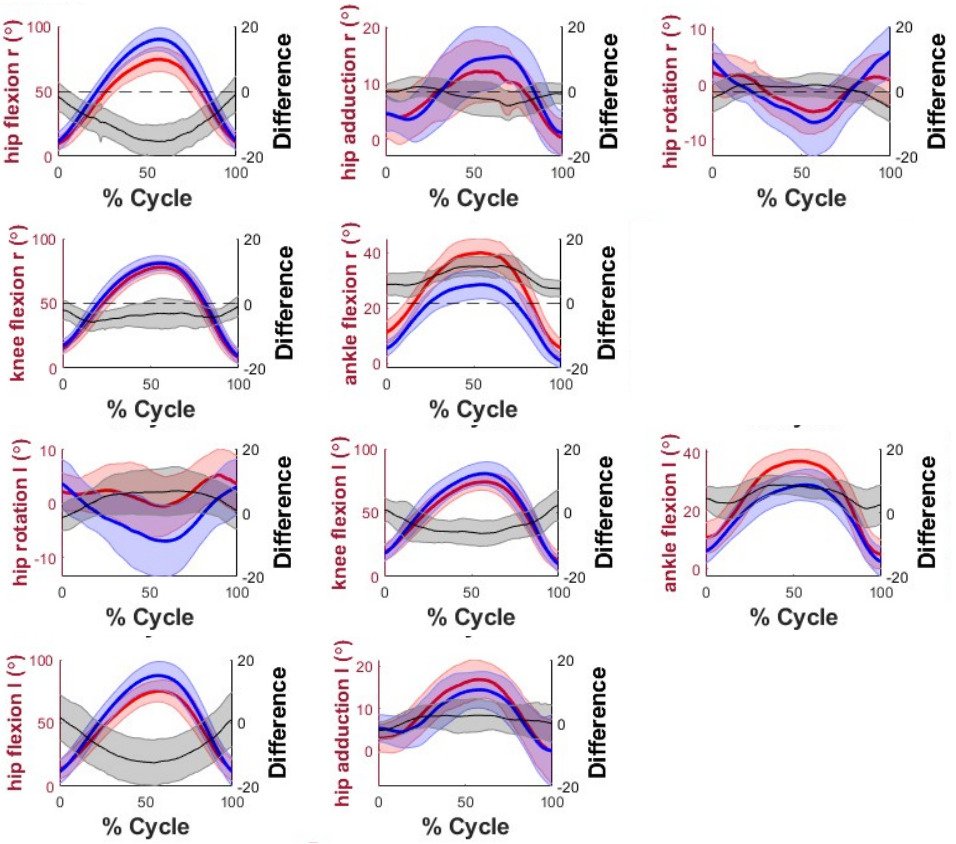

Figure 7.2, Continued

Counter-movement Jump

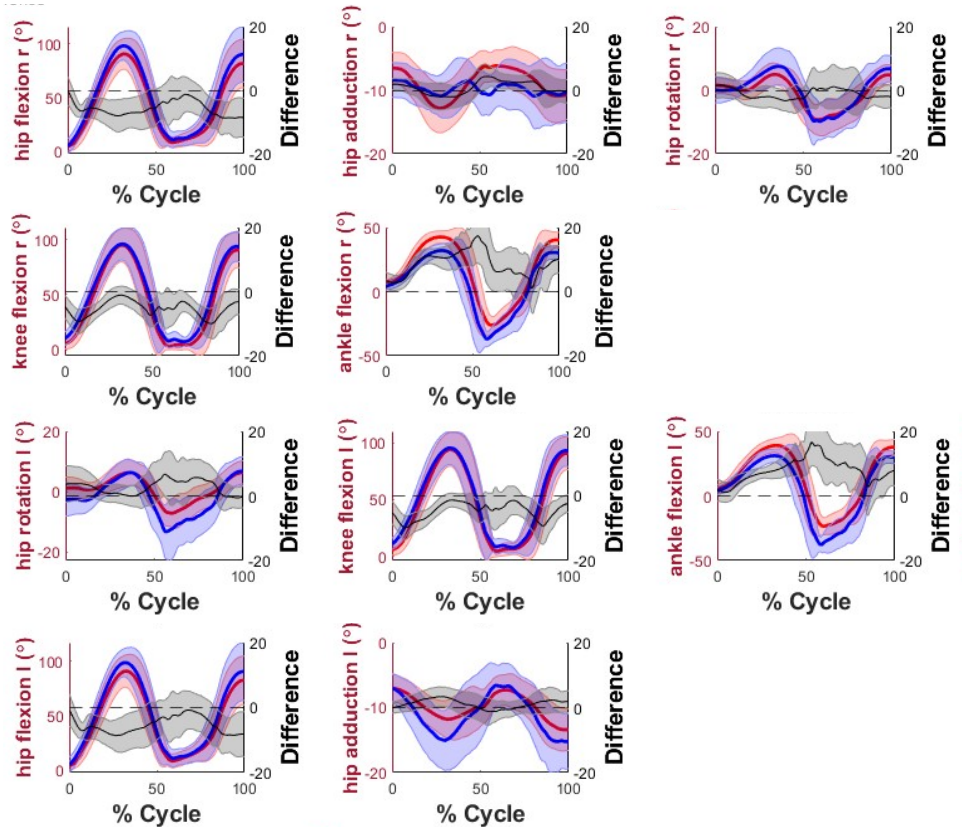

Single Leg Counter-movement Jump

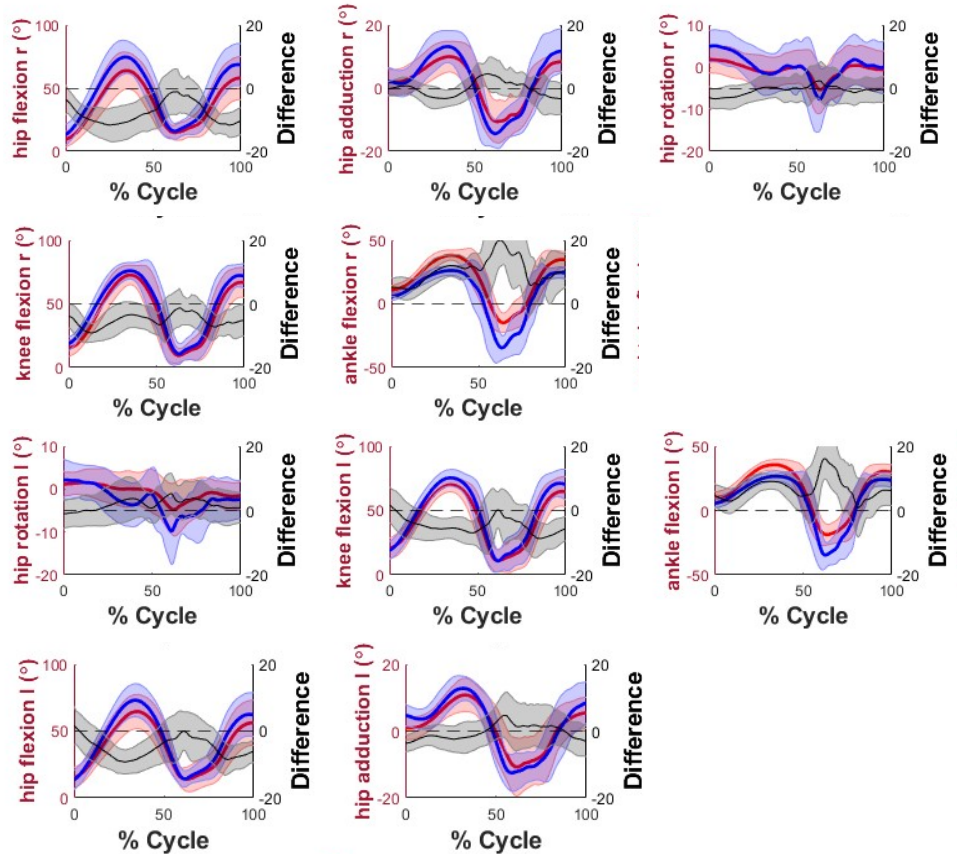

Figure 7.2, Continued

Drop Vertical Jump

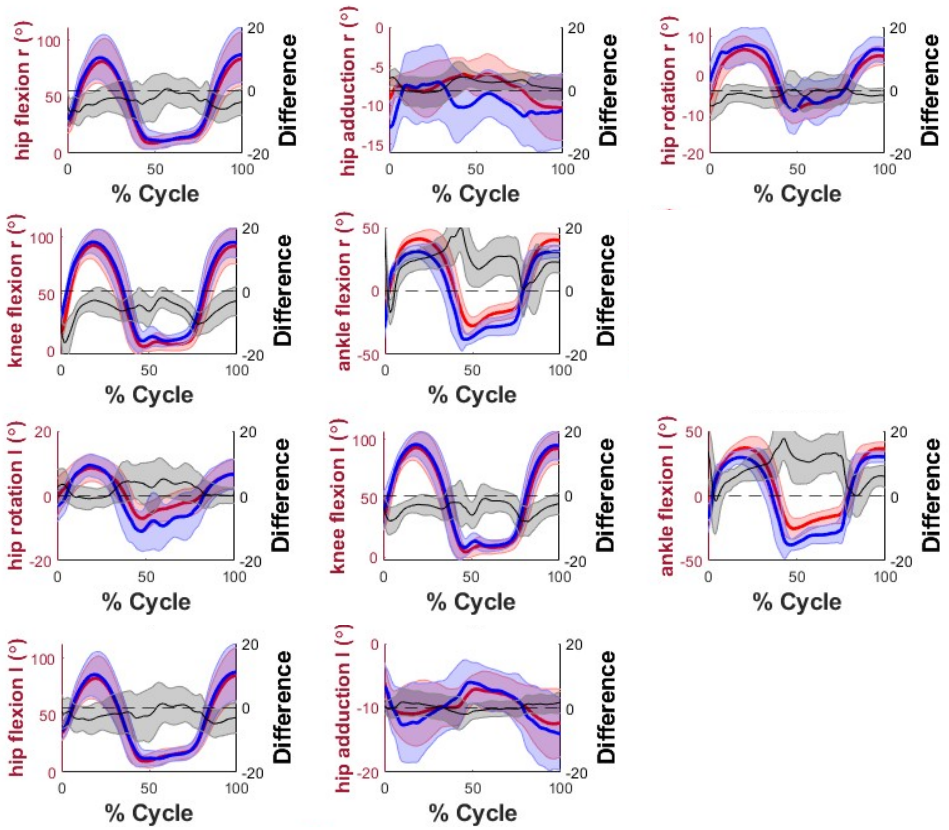

Single Leg Drop Vertical Jump

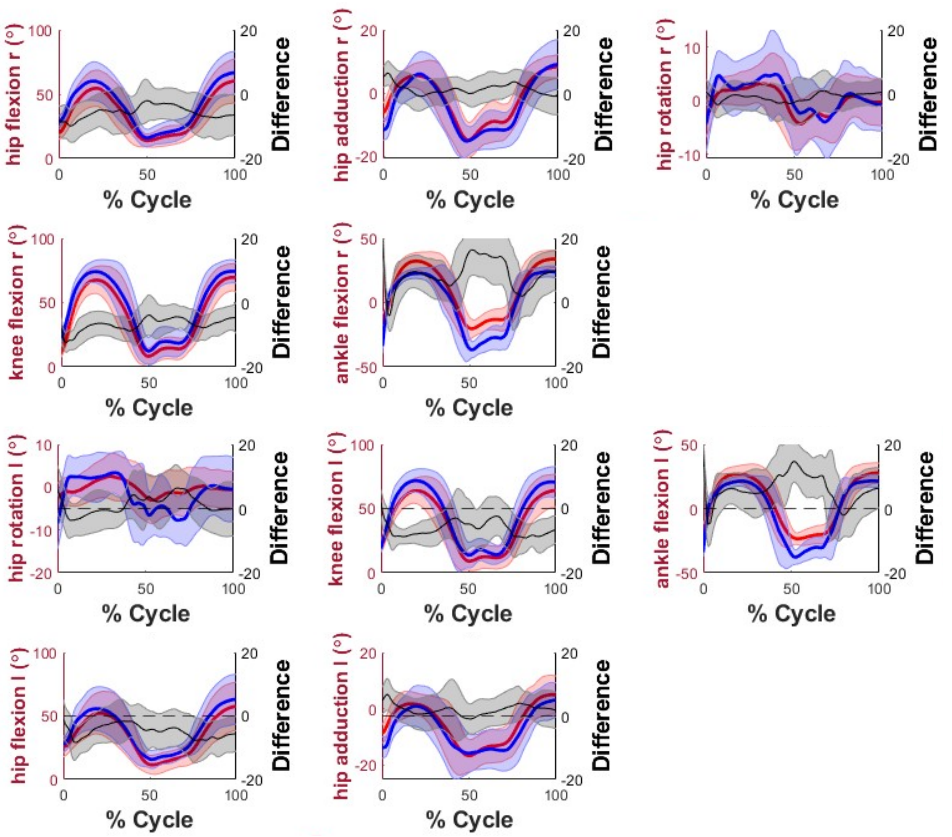

Figure 7.2, Continued

Heel Touch

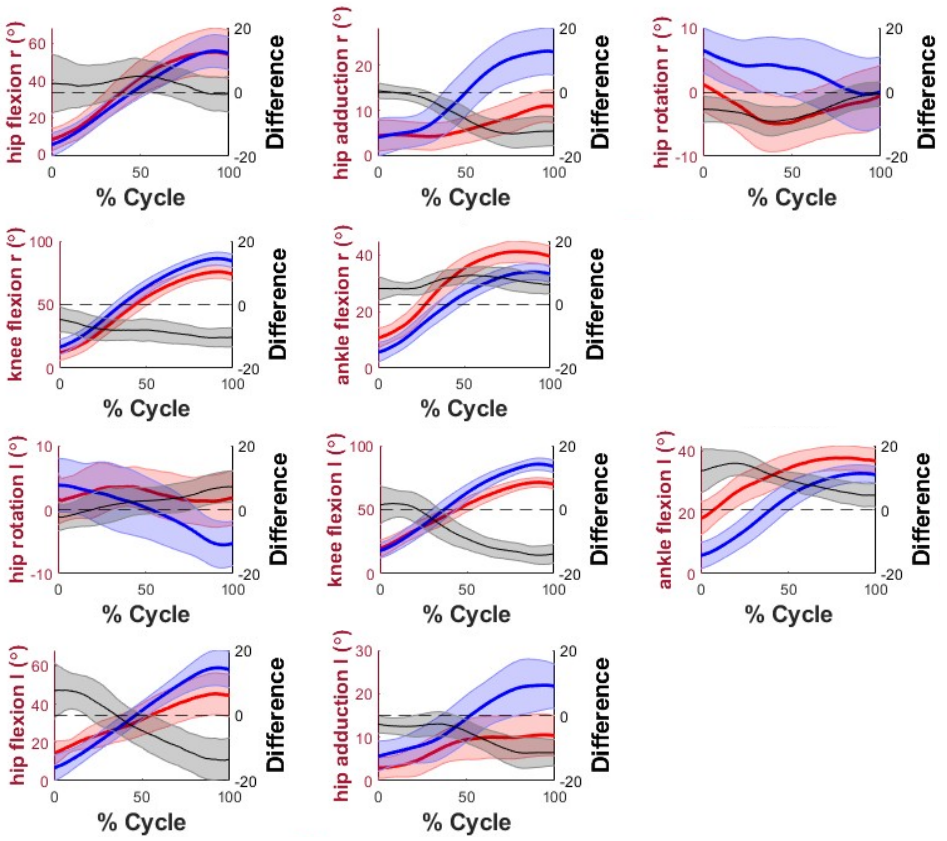

Lunge and Twist

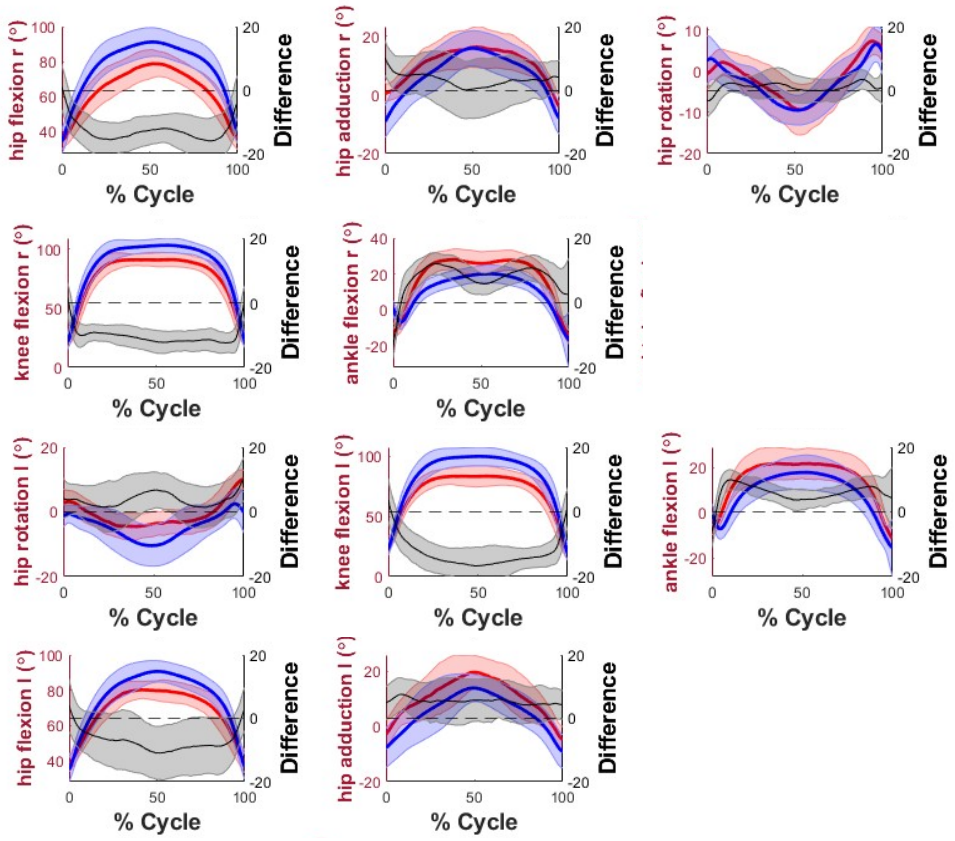

Figure 7.2, Continued

Single Leg Broad Jump